THIBHUVAN UNIVERSITY

INSTITUTE OF ENGINEERING

PULCHOWK CAMPUS

DEPARTMENT OF CIVIL ENGINEERING

M.SC PROGRAM IN STRUCTURAL ENGINEEERING

Thesis No:-SS00128

FINITE ELEMENT ANALYSIS AND FATIGUE DAMAGE CALCULATION OF WELDED BRIDGE –K JOINT

RAJENDRA SAPKOTA

April, 2009

THIBHUVAN UNIVERSITY

INSTITUTE OF ENGINEERING

PULCHOWK CAMPUS

DEPARTMENT OF CIVIL ENGINEERING

M.SC PROGRAM IN STRUCTURAL ENGINEEERING

Thesis No:-SS00128

FINITE ELEMENT ANALYSIS AND FATIGUE DAMAGE CALCULATIONOF WELDED BRIDGE –K JOINT

A thesis submitted by

RAJENDRA SAPKOTA

In the partial fulfillment of the requirement for the degree of

MASTER OF SCIENCE

IN

STRUCTURAL ENGINEERING

April, 2009

COPYRIGHT

CERTIFICATE

It is certified that the work contained in this thesis entitled "Finite Element Analysis and Fatigue Damage Calculation of Welded Bridge K-Joint" in partial fulfillment of the requirements for the degree of Master of Science in Structural Engineering, as a record of research work, has been carried out by Mr. Rajendra Sapkota (Roll No.063/MSS/R/109) under my supervision and guidance in the Institute of Engineering, Pulchowk Campus, Lalitpur. The work embodied in this thesis has not submitted elsewhere for a degree.

……..

Dr. Roshan Tuladhar
Co-ordinator in M.Sc. Structural Engineering
Department of Civil Engineering
Institute of Engineering, T.U
Pulchowk Campus
Nepal
April, 2009

ACKNOWLEDGEMENTS

I wish to express my profound gratitude to my supervisors: Dr. Roshan Tuladhar. Throughout the duration of the present study, he has given me invaluable guidance, criticism, suggestions, and encouragement. Honestly speaking, I used to refill my energy with the every active and friendly discussion with him every time I went to consult him, after some sort of frustration by continuously working for days and night but getting no solution. His enthusiasm and expertise was immersed into any little progress on my research work. For all of this, I will always be greatly appreciative.

I would like to express my deep sense of gratitude to the M.Sc program in Structural Engineering, Department of Civil Engineering, and Pulchowk campus for the financial assistances provided for the tour to the IIT-Kanpur at the initial stage of research work. It was really golden opportunity to get exposed to the precious literatures at IIT- Kanpur and the inspirational environment thereof including the interaction with respected professors: C.V.R Murty.

Also I would like to extend my appreciation to all my teachers who have brought me to this stage. I can never forget the contribution of respected expertise of structural engineering of the Department of Civil Engineering, Pulchowk Campus; especially Prof. Dr. P.N Maskey, Prof. Dr. M.P Aryal, Associate Prof. Dr. P.L Pradhan and Prof. Dr. Hikmat Raj Joshi or their valuable suggestions and encouragement at different stages of this research work.

My sincere thanks goes to my seniors and collegians of structural engineering and geotechnical engineering and all other helping hands for their kind cooperation during this research work especially Salik Ram Subedi, R.K Mallik, Bipin Shrestha, Deepak Gupta, Ranjit Lalchan, Nabaraj Baral and Sujan Tripathi.

I am also very grateful to my, family for supporting me throughout this entire process and allowing me to enjoy myself and have fun every once in awhile. Most importantly I am as usual, very much indebted to my dearest mother Mrs. Indira Sapkota, father, Krishna Prasad Sapkota, and brother, Deepak Sapkota for all their support, encouragement and loved which helped me every step of way. Without their understanding, encouragement and Support, I could not have reached on this stage. Finally I would like to thank my wife Sita Bastola, for her continued support, encouragement, understanding, patience and love.

Rajendra Sapkota
April, 2009

ABSTRACT

One of the most important deterioration mechanisms of steel bridges structures, which occur in service condition, is fatigue. In Nepal, numerous number of fatigue cracks has been recently reported to initiate in steel bridges in superstructures and even in sub structures. Such fatigue cracks may lead a significant influence to the traffic and even collapse of the bridges if the cracks are left to propagate. Repair and retrofitting works including investigation of fatigue mechanism for such fatigue damage are very urgent issues now. This is the research work about the finite element modeling and fatigue damage calculation of steel welded truss bridges. The Rapti Bridge of Nepal is taken as a typical case that was failed by buckling and retrofitted by welding technique.3D finite element model of Rapti bridges was created using the available SAP2000 software package. The result obtained from the linear analysis was used to find the most critical joint for fatigue damage. The analysis shows that the middle joint is the most critical joint for IRC class –A load.

For the modeling of k- joint and calculation of fatigue damage the software package ANSYS Ver.10 was used. The micro model of the k joint was model using the elements available in software package. In the FE model, 3D 20 node tetrahedral solid elements, solid 95, was used for gusset plate and diagonal members. The weld nugget was model using a two node beam element BEAM 188. Contact and target elements, Targe170 and Conta175 were also created on the inner surfaces of the plates around the weld. The transient step loading analysis was done considering the effect of material non linearity. In the present study, numerical analysis was carried out to look into the performance of welded k- joint in axial loading with different weld radius. Strength of joint is increased with the increase of weld radius. The displacement along the longitudinal direction is decreased and the stress distribution is more uniform with the increases of weld radius. The stress life approach (S-N) curve was used to evaluate the cumulative fatigue damage. Based on the predicted stress and strain states fatigues life analysis were performed. The result of this study shows that the fatigue life of welded joint increases with the weld diameter. In this study, the weld radius 5mm has a lesser fatigue damage than the weld radius 3mm and 2mm.

TABLE OF CONTENTS

LIST OF FIGURES

LIST OF TABLES

NOTATIONS

Roman Notations	Meaning
BC	Bottom chord
TC	Top chord
E	modulus of elasticity
fy	yield strength
HAZ	heat-affected zone
Kt	theoretical stress concentration factor
ΔK	range of stress intensity factor
m	material dependent constant
n_i	number of cycles applied
N_i	number of cycles required to failure
N_p	fatigue crack propagation life
R	stress ratio
S	nominal stress
ΔS	range of stress
S_a	alternating stress
S_m	mean stress
υ	Poisson's ratio
HCF	High cycle fatigue
S_e	Endurance limit
S_u	Ultimate Strength
WRS	Weld radius stress
IS	Indian code

1. INTRODUCTION

1.1 Background

Fatigue in bridges has been a concern to the transportation community for many years. Reinforced concrete bridges are not always possible to full fill the need of large span and in case of emergency. Pre stressed bridges is an alternative way to cover the large span but not being practiced in the country. In such situation, steel truss bridges can only be the alternatives. Bolts and welds are the main connecting elements in the joint of steel bridges.

Bridge fatigue can be a serious problem. If ignored, fatigue can cause sudden and total failure of a bridge. Fatigue failure of a detail can occur at stress levels far below the ultimate strengths of that material. Fatigue failure is dependent on time and frequency of loading; moreover, failure occurs due to the repeated cyclic loading of a structure. Fatigue failure is an important consideration in older bridges that have experienced a larger number of loads cycles and are more susceptible to failure at lower stress ranges than newer bridges that have not been exposed to as many cycles. The time it takes for a structure to fail due to fatigue is called the fatigue life. Fatigue life can be calculated throughout the life of a structure.

Stress concentrations at the weld toe and root are caused by the geometrical discontinuities and, thus, fatigue cracks are easily initiated at these locations. Stress concentrations may also result from weld defects, e.g., at weld toe from cold laps and undercuts, and at the weld root from incomplete fusion and small effective throat thickness. A significant feature of fatigue is that the load is not large enough to cause immediate failure. Fatigue failure is still a dominating cause for breakdown of welded structures in construction and mining equipment, trains, ships, agricultural machinery, bridges and off shore equipment.

In the context of engineering, fatigue is defined as a process of cycle by cycle accumulation of damage in a material undergoing fluctuating stresses and strain. Instead, failures occurs after a certain number of load fluctuating have been experienced. The fatigue process can generally be broken into two distinct phase:

crack initiation and propagation. The crack initiation life is usually short in welded structures because can always be assumed that the sharp edges discontinuities exists in welded structures.

Three general methods of fatigue analysis are used in structural analysis and design. They are stress life, strain life and linear elastic fracture mechanics. The most widely used and most straightforward tool for structural stress analysis and analyses is the finite element method. When it comes to finite element modeling simulation of the welding process in order to study the heat transfer, deformation and stresses many phenomena have to be considered. Despite several simplifications, neglecting the micro structural changes during heating and cooling, lack of material decelerated temperatures and constant heat source modeling, finite element modeling is still a complex task.

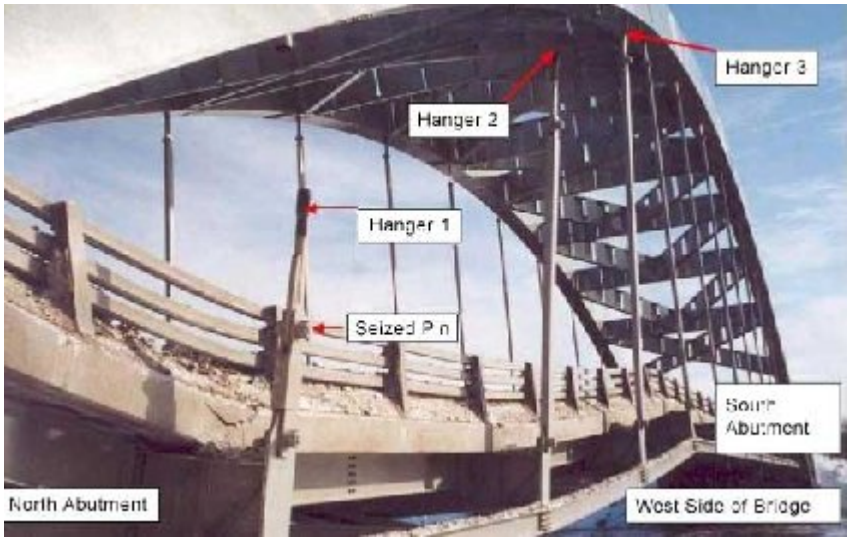

Figure 1.1: Fatigue failure of V.C Memorial Bridge over the Montreal River at Latchford: January 14, 2003 [Dino Bagnariol]

1.2 Need of Research Work

One of the most important deterioration mechanisms of steel bridge structures, which occurs in-service condition, is fatigue. Since from 1960 a number of bridge structures in America and Europe have experienced fatigue cracking which sometimes results brittle fractures, fatigue problem in steel bridges has been started to be investigated. There are many cases of serious fatigue failure i.e. failure of the Sgt. Aubrey Cosens VC Memorial Bridge was caused by the fatigue-induced fracture of three steel hanger rods on the northwest side of the bridge in January 14, 2003 in Ontario, failure of the Tacoma Narrows Bridge in Washington state near to Puget Sound in USA in 1999.

In Nepal, numerous number of fatigue cracks has been recently reported to initiate in steel bridge superstructures and even substructures. The news published in Kantipur daily in Friday, March 6, 2009 on title Ninety Percent of Bridges are in endanger in Nepal mention that there are around fifteen hundred bridges in country. Ninety percent bridges are older than twenty five years. Almost thirteen hundred fifty bridges are near to failure at any time in the absence of rehabilitation. The above data contains the minor and major steel bridges which are located in national highways. Most of the bridges are bolted connections. But if we have to retrofit it welding is necessary. The evidences of that can see in Rapti Bridge in Nepal. It is fact that welded joints are particularly vulnerable to fatigue damage when subjected to repetitive loading. Fatigue cracks may initiate and grow in the vicinity of the weld during services life even if the dynamic stresses are modest and well below the yield limit. In addition, when cracks occur in the vicinity of welded structures, weld repairs are frequently considered for crack repair, in most cases, to extend service life. It is necessary to know and be able to assess whether, and to what extent, weld repair processes can improve fatigue life of cracked welded structures.

Since such fatigue cracks may lead a significant influence to the traffic and even collapse of the bridges if the cracks are left to propagate, repair and retrofitting works including investigation of fatigue mechanism for such fatigue damaged bridges are very urgent issues now.

In this study it will try to make FE model of bridge k- joint which represents actual behavior and fatigue damage calculation of welded joint.

1.3 Objective of Research Work

In overall, this research aims at carrying out the finite element analysis of welded bridge k- joint and basic understanding of the fatigue behavior of the welded joints based on the theoretical considerations. The following are the major objectives that would correspondingly address the problem and issues floated earlier.

1. To develop the suitable Finite Element Model of welded bridge-k joint.
2. To understand the behavior of welded bridge-k joint in dynamic axial loading.
3. To evaluates the fatigue damage of welded gusseted joint numerically.

1.4 Scope of the Research Work

A bridges structure is very complicated structure in itself and its accurate fatigue analysis need advanced knowledge on fracture mechanics and fatigue loading. However, the present research focus on modeling and evaluation of fatigue damage from the point of view of structural engineering and follows the simplified techniques. Some specific points regarding the scope of this research work are listed below:

1. The stress life approach is used to evaluate the fatigue damage.
2. The channel sections used in bridge are model as a rectangular section in FE model.
3. The fatigue damages are calculated based on the axial load only.
4. The analysis is carried out only for IRC class –A loading.
5. Non linear analysis is carried out using elastic perfectly plastic constitutive law.
6. Weld residual stress, welding techniques and distortion produced in welding, lack of fusion, undercut, solidification crack, porosity and misalignment are beyond the scope of my research work.
7. Experimental verification of the numerical analysis is beyond the scope of this research.

1.5 Organization of thesis

The main body of this research is divided into seven chapters, and they almost reflect the sequences of the progress followed by. Chapter1 gives the idea on the importance of steel bridges in case of Nepal .It briefs on the objectives and the scope of the research on the finite element analysis and fatigue damage calculation of welded bridge k- joint. Chapter 2 the literatures reviewed on the various aspects of the finite element. Chapter 3 is allocated for the numerical modeling, which describes on geometry of bridge joint, the material property, boundary condition, and material property. Chapter 4 devotes to the numerical analysis of the model worked in the chapter 3.Chapter 5 contains the results and discussions of the numerical analysis. The conclusions thus derived from these investigations are given in chapter 6. A great deal of potential extensions to the present research is explored which is recommended in chapter 7 for future works.

2. LITERATURE REVIEW

2.1 General

Metal fatigue, which results in fatigue crack, is the process of premature failure or damage of a component subjected to the repeated application of loads which individually would be too small to cause failure. Fatigue cracks usually initiate on the surface of the component on the microscopic scale and they are referred to as crack initiation or stage I cracks. During the fatigue life, crack growth usually occurs on the macroscopic scale in the direction normal to the applied tensile stress, and it is referred to as crack propagation or stage II. Finally, the component may fail due to fracture.

Earlier fatigue theories analyzed the entire fatigue life of a component as a single entity. However; modern fatigue theories analyze each of the three stages of fatigue life separately. This is typically accomplished by splitting the fatigue life into two periods: the crack initiation period followed by the crack propagation or growth period. It is very difficult if not impossible to define the transition from initiation to propagation of crack growth due to the variability.

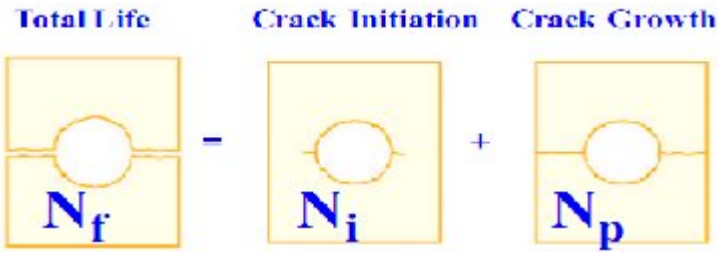

Figure 2.1: Different phase of fatigue damage

2.2 On The Problem Formulation

2.2.1 Stress –Life Approach

The stress-life approach was first introduced by Wholer in the 1860's and presents a menas of detrerminig the fatigue life of a smooth specimen subjected to an aplied alternating stress. This emperical method is best suited for high cycle fatigue(HCF)

and introduces the concept of an endurance or fatigue limit.This traditional approach was developed in its present form by 1995 and it is based on the nominal stresses in the region of the component being analysed.

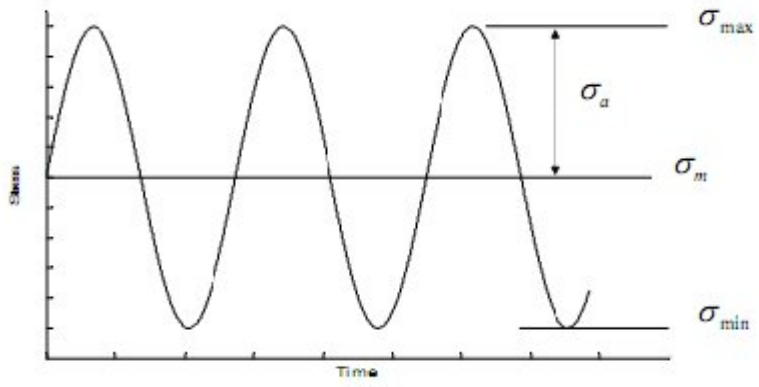

Figure 2.2: constant Amplitude Cycle Terminology [Wohler 1960]

Several parameters must first be defined in order to discuss the stress- based approach for fatigue. These parameters are shown schematically in figure2.2 which shows a sinusoidal waveform of a fatigue cycle. The stress rang, $\Delta\sigma$, the stress amplitude, σ_a and the mean stress, σ_m are defined as:

$\Delta\sigma$ = - , $\sigma_a = \frac{}{}$, $\sigma_m = \frac{}{}$

Additionally, ratios of the parameters are often used and defined by:

$R = \frac{}{}$, $A = \frac{}{}$

Where R and A are the stress and amplitude ratios, respectively. With the stress ration defined in this manner, fully reversed loading occurs when R= -1, zero – to-tension fatigue occurs when R=0, and static loading occurs when R=1.

2.2.3 S-N Diagrams

The basis of the stress-based method is the stress-life curve, also called the S-N diagram, where the amplitude of stress (σ_a)or nominal stress (S_a) is plotted versus the number of cycles to failure, N_f. The number of cycles to failure is usually plotted on a logarithmic scale since the cycle numbers change rapidly with the stress magnitude. Two distinct types of S-N behaviour are represented sschemetiacally in figure 2.3.As

these figures imply,higher stress magnitudes result in reducing the number of cycles that the material is capable of sustainig before failure. Additionally, some ferrous materials, such as plain carbon and low –alloy steels,exhibit a distinct endurance limit (S_e), where the S-N curve becomes flat and asymptoticaly approaches the stress amplitude of S_e. However, for materials such as aluminium and copper alloys, the S-N curve does not appear to appraoach an asymptote. Thus the fatigue limit is specified by the fatigue strength and defined by the stess level at which failure will occccur for a specified number of cycles, typically defines between 10^7 and 10^8cycles. The endurance limit for most ferrous materials is often related to the ultimate strength(S_u) of the material.

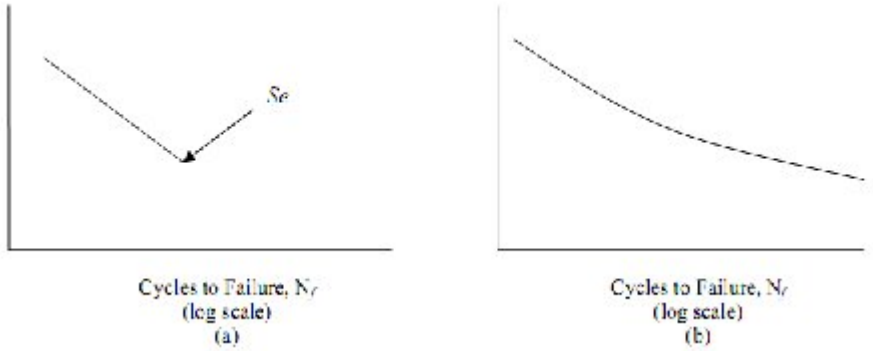

Figure 2.3: S-N curves for (a) Material displaying a Fatigue limit and (b) Material Not Displaying a Fatigue Limit

The data points of the S-N curve are determined experimentally from an unnotched specimen under constant amplitude loading with a zero mean stress, or at some specific non zero mean stress, σ_m. The test is repeated at increasingly higher stress levels equating to lower cycle to failure. During the development of S-N curves it is not uncommon to observe an order magnitude uncertainity in statistical scatter of the test data. The resulting S-N curves consists of averaging the number of life cycles for each applied stress level. A linear relationship of the averaged curve is commonly sbserved on a log-log plot with the mathematical representation of the obtained by the following equation:

$$\frac{}{} = \sigma_a = \sigma_f'(2N_f)^b$$

Where σ_f is the fatigue strength coefficient and is often approximately equal to the true fracture strength σ_f and b is know as the fatigue strength exponent or Basquin exponent. Both σ_f and b are the fatigue propertiese of the material.Lastly,$2N_f$ or half – cycles is the number of reversals to failure and N_f is the number of cycles.

2.2.4 Mean Stress Effects

Thus far, the empirical description of the fatigue life pertains to fully reversed fatigue loads where the mean stress of the fatigue cycle, σm is equal to zero.However, this is not necessarily representative of many applications where in fact the mean stress may not be equal to zero. The fatigue behavior of engineering materials is known to be greatly influenced by the mean level, where typically a mean tensile stress is more detrimental than a mean compressive stress. It has been observed that increasing the mean stress level decreases the fatigue life.

Mean stress effects in fatigue can be represented by constant-life diagrams, as shown in Figure 2.4. Stresses falling above the possible failure criteria lines result in failure. The most well known failure models are the Gerber line and the Modified Goodman line which are best used for fracture criteria, and the Soderberg line which is best used for yield criteria.

The failure models are described by the following equations:

Gerber(1874) : $\frac{}{} + \left(\frac{}{}\right)^2 = 1$

Modified Goodman(1899): $\frac{}{} + \frac{}{} = 1$

Soderberg(1939): $\frac{}{} + \frac{}{} = 1$

Morrow(1960): $\frac{}{} + \frac{}{\sigma} = 1$

Where:

Sy = the yield strength

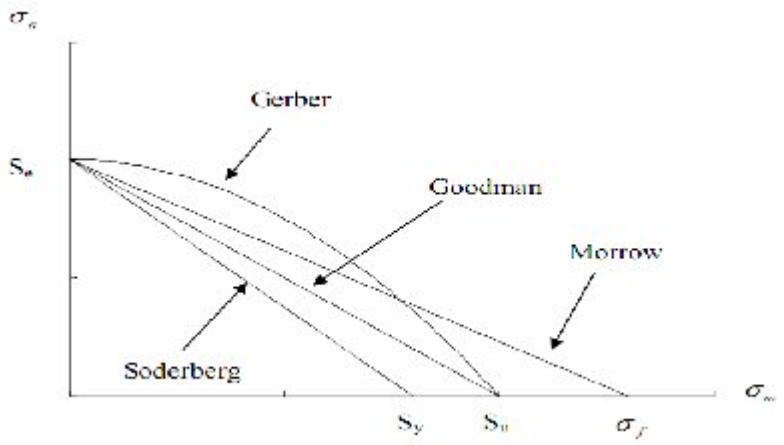

Figure 2.4: Comparison of constant Life curves

Where Sa is the alternating stress, S_m is the mean stress, S_f is the fully reversed fatigue strength of the specimen, S_{ut} is the tensile strength. There is controversy on how the equivalent stress should be calculated. Use of maximum principal stress was suggested as representative of equivalent alternating stress.

For equivalent mean stress

$$S_{em} = \sqrt{\quad} \quad \sqrt{\quad} \quad \sqrt{\quad}$$

Here σ_{a1}, σ_{a2}, σ_{a3} are principal alternating nominal stress with $\sigma_{a1}>\sigma_{a2}>\sigma_{a3}$.

Or sum of normal mean stresses

$$S_{em} = \sigma_{m1}+\sigma_{m2}+\sigma_{m3} = \sigma_{mx}+\sigma_{my}+\sigma_{mz}$$

Some general observations can be made on the failure criteria models when discussing cases of tensile mean stresses. The Gerber model is generally appropriate for ductile alloys but does not distinguish between tensile and compressive mean stresses. The Modified Goodman model is best suited for brittle metals. It is generally conservative for ductile alloys and it is generally non-conservative for compressive mean stresses. The Soderberg model is seldom used since this method is very conservative for most alloys.

2.2.5 Modifying Factors

Several modifying factors are usually considered when using the stress-based approach for fatigue analysis of a smooth unnotched test specimen. Years of testing of the effects of various factors such as: surface finish and treatments (k_a), size (k_b), loading (k_c), temperature (k_d), and other miscellaneous effects (k_e) such as the environment have been quantified as modification factors that result in a modified endurance limit often denoted as S_e . The modified endurance limit tends to be conservative with a correction for the remainder of the S-N curve not clearly defined. The modified endurance limit has the form:

$$S_e' = K_a K_b K_c K_d K_e S_e$$

The endurance limit will typically be reduced by the tensile mean stress, large section size, rough surface finish, chrome and nickel plating, decarburization (due to forging and hot rolling) and severe grinding.

2.3 Cumulative Fatigue Damage method

An engineering component's total life can be defined into crack initiation and propagation stages. Thus, there are different approaches used in determining cumulative fatigue damage in regards to the safe-life and damage tolerant approaches for fatigue.

2.3.1 Miner's Rule

The linear cumulative damage hypothesis was first proposed by palmgren as early as 1924 and further developed by Miner in 1945. This empirical damage summing method for the initiation phase as determined by either the stress or strain life approaches is best known as Miner's rule.

The load history as shown in figure 2.5 consists of two blocks of constant amplitude loading making up a variable amplitude load history. If the loading consists of only the largest cycles and it is assume this load history will be repeated until failure the engineering component will be exposed to a constant amplitude load history. Failure as defined by Miners' rule occurs when

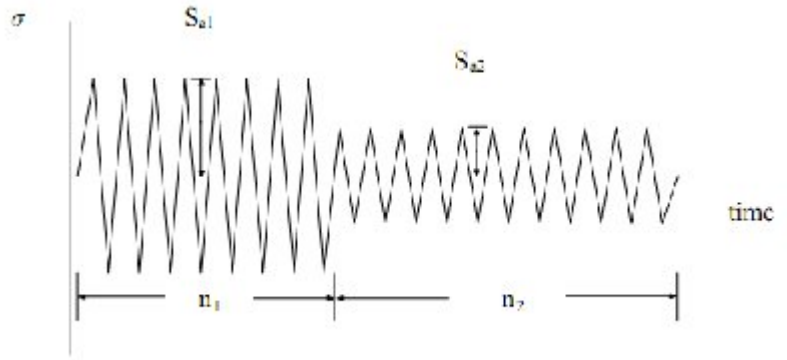

Figure 2.5: Palmgren-Miner Rule for Life Prediction of Variable Amplitude Loading

—= 1

Where

n1= the number of cycles at stress level s_{al}

N1= the number of cycles to failure as obtained from the fatigue life endurance limit.

The failure criteria for variable amplitude loading is simply the summation of the life fractions for each loading blocks, thus damage (B_f) is defined as

B_f = — + — + — +……. = — =1

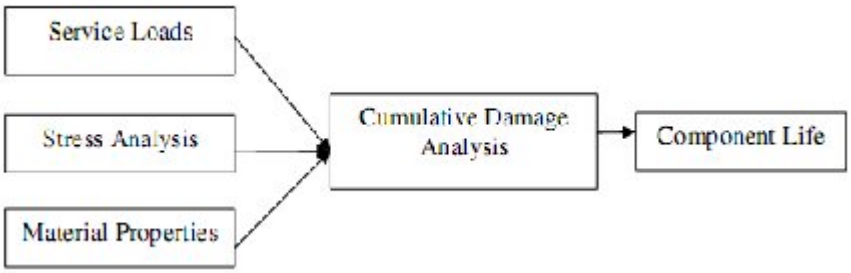

Figure 2.6: The Cumulative damage analysis

2.4 Concluding Remarks

The S-N method is quite simple method and can be used in almost any situations to obtain an initial estimate of the fatigue life. The methods works well in applications of constant amplitude loading and designs involving long fatigue lives. There are many existing S-N and test data readily available. However, this method is completely empirical and it derives from tensile tests of materials in the intermediate to long life region. Additionally, this method ignores plastic strains, which are critical for short fatigue lives, and this method is often dependents on geometry.

2.5 On Finite Element analysis Specific Research on Fatigue Life Calculation

2.5.1 Finite Element Model and Analysis of Fatigue Damage

Hanifi and Onder, (2007), a parametric study on the fatigue life behavior of spot welded joints, studied the fatigue life values for four different types of spot weld diameter. The result of his study shows that the fatigue life of a spot welded specimen dependent most significantly on the type of specimen, applied amplitudes and off course the spot weld diameter. Failure in a spot-weld occurs in the heat affected zone (HAZ) of unmolded metal between the base metal and the weld metal. The HAZ is subjected to higher stresses than the surrounding base metal and is the location of failure in most cases. The failure modes for tensile and modified tensile loading cases depended primarily on the magnitude of the applied mean load and the nugget diameter.

Rahaman, et.al, (2008), fatigue life prediction of spot welded structures: A finite element Analysis Approach, studied the effects of sheet thickness and weld diameter. A simple model was used to illustrate the technique of spot weld fatigue analysis. Finite element model was built for different sheet thickness and weld radius. And analysis was carried out using utilizing the finite element commercial codes. It observed that the fatigue life of the structure increases with the increases of the spot weld diameter and sheet thickness.

2.5.2 Fatigue Crack Growth in Welded Joint

Considering fatigue crack growth in welded joints, the percentage of the crack propagation phase in the total fatigue life is very much dependent on the quality of the weld comprising weld geometry, initial defects in the weld, weld residual stresses and local stress conditions. Since welding defects can frequently exist in the vicinity of weldments, local stress concentrations around discontinuities and weld defects are fairly common. These crack-like defects begin to grow almost immediately when subjected to external cyclic fatigue loads, so that, for welded joints, the total fatigue life is mainly dominated by the crack propagation phase.

Wu, (2002), measured the crack growth rate during constant amplitude fatigue testing on un-welded, as-welded and weld repaired specimens of 5083-H321 aluminum alloy. A 3-D finite element analysis was conducted to determine the stress intensity factors for different lengths of crack taking into account the three-dimensional nature of the weld profile. It was found that crack growth rates in welded plates are of the same order of magnitude as those of parent material when effective stress intensity factors were applied.

Bell and Vosikovsky, (1992), conducted research work on the fatigue crack initiation and propagation behavior for multiple cracks in welded T-joints for offshore structures. They showed that many semi-elliptical cracks initiate along the weld toe and progressively coalesce as they divided into fewer large cracks. It was also noted that crack coalescence accounted for a significant portion of the propagation life.
Ferrica and Branco, (1990), investigated the effects of weld geometry factors on the fatigue properties of cruciform and T-weld joints. The results showed that the thickness of main plate and the radius of weld-toe are the most important factors for the fatigue properties of welded joints.

Murthy et al., (1994), investigated the fatigue crack initiation and propagation behaviors of welded steel tubular structures. The results obtained indicated that the crack growth life was 75% to 89 % of the total life for all the welded joints tested. It has been confirmed by other researchers [Kapadia, 1978, Masubuchi, 1980,

Nagamoto et al., 1987] that tensile residual stress can significantly decrease the fatigue properties on welded joints.

Nagamoto et al., (1987), studied fatigue crack growth behavior of Al-5083 base and MIG welded plates. It has been shown that the crack growth in the base material was faster than in the welded specimens.

Linda (1990), investigated fatigue crack growth behavior in butt weld joint of Al-5456-H116 aluminum alloy and ASTMA 710 steel. Crack closure levels were determined graphically using the upper tangent point, and non-subjectively by measuring the 2% deviation from the upper linear portion of traces. The experimental results showed that the da/dN curve, when using the effective stress intensity factor range, shifted to faster growth rates in welded plates compared to the base plate. Crack closure loads of up to 80 % of the maximum load were measured in both Aluminum and steel welded specimens. These closure levels were mainly created by the presence of weld residual stress (WRS). For stress relieved steel specimens, the fatigue growth rate shifted to rates equivalent to those of the base plates.

It was concluded in the paper that applying effective stress intensity factor, taking into account of weld residual stress effects, results in more accurate estimations of fatigue life in welded joints.

2.5.3 On Welding Design and Fatigue Design Guidelines

Is 1024:1999 Indian Standard Use of Welding in Bridges and Structures Subjects to Dynamic Loading is the reference code for the present study. The permissible stress shall in no case exceed the stresses permitted in the relevant Indian Standard Specifications. Since the fatigue strength of welded structures depends upon the constructional details, these shall be decided before the permissible stresses and consequently the size of members and weld sizes are determined. The value of maximum allowable tensile or compressive stress (f) and allowable number of repetitions of this stress cycles (N) for fluctuating stresses – class F constructional detail are taken. The data for class F constructional detail is given in appendix F.

3. FINITE ELEMENT MODELING

3.1 General

Finite element analysis (FEA), also called the finite element method (FEM), is a method of analyzing engineering components in which the geometry of the structure of discredited into a series of nodes and elements. Using these numerical techniques, a solution in terms of stresses, strains, deflection, temperatures and frequency can be obtained. These results, in turn, can be used for fatigue analysis. Fatigue analysis software uses stress result from FE analysis.

Fatigue analysis from FEA models is a fairly new subject, and many of the analysis rules have yet to be established. However, since crack initiation predominately occurs on the surface of a component, nodal stresses are generally the preferred approach over integration point stresses and averaged elemental stresses. Additionally, life prediction is dependent on the accuracy of both the stress analysis and the fatigue damage analysis. Chu, (2004) has stated that a 10% error in the stress calculation is likely to double the error in the calculation of fatigue damage. Therefore, careful attention must be given to geometry details, mesh density, load history, and material properties. In a typical FE analysis, elements are joined at nodes, with each node having several values of stress calculated from adjacent elements. FE codes generally average these stresses, resulting in a single average nodal stress tensor for each node in the model. A good indication of the quality of the mesh is the difference between the averaged and un-averaged stresses at a node.

To ensure that Miner's Rule gives adequate life estimates for most engineering applications, fatigue analysis codes reduce the stress or strain amplitude at the endurance limit, which is determined from a constant amplitude test by 20% to 25%. This has become a common practice since under variable amplitude loading the endurance limit may disappear or its amplitude may be reduced. Fatigue software is used to calculate the time histories of the in-plane principal stresses and their corresponding directions at the surface of the model. The strain time history is

then used in a strain life fatigue calculation and the process is repeated for each node in the model (Draper. Aveline R. 2004 USA)

Major advances have been made in fatigue analysis software over the past decade and the correlation between predicted fatigue life and fatigue life based on test results are improving. Software such as ANSYS and FE-Fatigue are able to predict hotspots and actual fatigue lives with relative accuracy and reasonable processing speed. This is accomplished using either the stress-life method or the strain-life method. Once the hotspots are determined the results can be exported back into a FEA code to determine crack propagation and fracture if necessary. The commercial finite element software ANSYS was chosen for the implementation of this K-joint connection model because of the flexibility it provides in defining the connected different parts in FE level and local material constitutive law.

3.2 Introduction to ANSYS

ANSYS is three dimensional finite element analysis commercial tools that can be used for a range of structure. ANSYS structural provide all the power of ANSYS nonlinear structural capabilities-as well as linear capabilities in order to deliver the highest quality most reliable structural solution. A full complement of non linear and linear material laws and inelastic material model is provided in this software. It not only offers the fanciest intuitive, tree- structured GUI for easy definition of complicated shape modeling.

Through identifying the key-points, lines areas and volumes, either of the methods can be building up a 3-d model by themselves. By using the mapping tools provided by the software, a well defined mesh can be established based on the geometry of the volume. On the contrary, the ANSYS code had the well organized input from and can identify the exact points as many as possible. Both static and dynamic analysis are included in the ANSYS package.

Preprocessor is the first step for a fatigue analysis. The step consists of creating the model and mesh specifying the material properties, load and boundary conditions. Solution is the second step which consists of selecting the analysis type and then

solution. General postprocessor is the third step which consists of results summary, option for output, result viewer, fatigue calculation module etc.

3.3 General Description

There was a great deal of detail involved in the creation of three dimensional models of full scale K- joint. In an effort to provide an organization overview of the steps involved in the model development, this chapter is separated in to five main sections: General Description, Welding design, Finite Element Model, Load and Boundary Condition.

3.3.1 Geometry of the bridge

In order to accomplish the mission of this research, a typical bridge, Rapti Bridge along the road of lamahi-koilabash in dang district in Nepal was taken. This is a deck through type Bridge of total length 300m with six spans. Each span is 50 m having 10 panel 5 m each. This is a single lane bridge designed under IRC class -A loading. Structural steel conforming to IS 2062-1999 with ultimate stress of 410 MPa as mentioned in the supplied drawing has been used. The yield stress for such steel as stated in literatures is 280 MPa. Structural system of bridge consists following components

- Bottom chord –ISMC 400
- Top chord –ISMC 300
- Diagonal member – ISMC 300 and ISMC 250
- Top and bottom bracing – pair of ISA75*75*6
- Cross beam – ISMB 400
- Stringer beam –ISMB 400
- Gusset plate – 6mm to 10 mm
- Joint and connections- The top and bottom joint of the main truss element are connected together by splice joints. Splice joints are provided at a distance of about 10 m. Panel joint is also provided between the splice joint.

3.3.2 Welding design

The length of weld required to resist the given force is calculated using the IS 816-1969 (fourteenth revision October 1997). The length of weld calculated is used only for micro model of k joint. The length of weld was calculated for bottom chord and diagonal member using IS code.

The effective throat thickness of a weld is the perpendicular distances from the root to the hypotenuse of the largest isosceles right triangles that can be inscribed within the weld cross-section. The effective throat thickness of a fillet weld shall not be less than 3mm and shall generally not exceed 0.7t and 1.0 t under special circumstances where t is the thickness of the thinner part.

Effective throat thickness = 0.7* size of weld

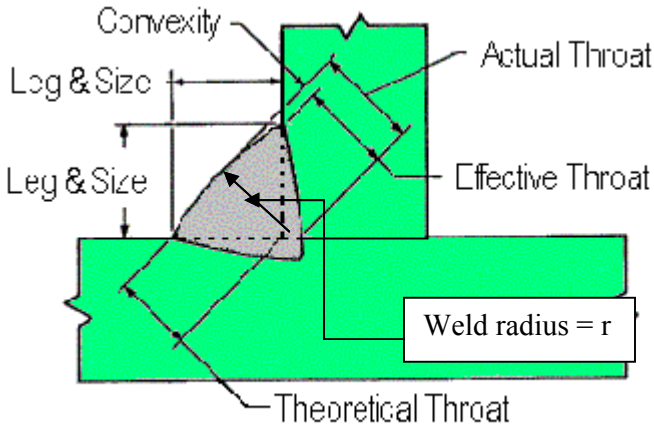

Figure 3.1: Weld radius define in ANSYS

3.3.3 Finite Element Model

The following paragraph in this section will outline the modeling techniques used and the development of each component of the finite element models. This component includes the gusset plate, bottom chord and diagonal member.

3.3.4 Model Description of k- joint

In the FE model, a 3D 20 –node tetrahedral solid element, SOLID95, was used for the gusset plate and, bottom chord and diagonal members. This element has plasticity, stress stiffening, large deflection, and large strain capabilities. On the other hand, the nugget was modeled using a two node beam element, BEAM188. Contact and target elements, Targe170 and cont175, were created on the inner surfaces of the plates around the weld. The beam element, BEAM188, is based on Timoshenko beam theory. Shear deformation effects are therefore included, which are especially important for short beams. This element has a six degree of freedom at each node. The nugget experience low stresses, its material model was chosen as linearly elastic.

In welding process, heat treatment does not affect the mechanical properties of the material. Therefore, it is necessary to use the material properties for the nugget and base material. Therefore, it is necessary to use the same material properties for the weld nugget and the base metal. Hence in this study, base metal and weld are modeled using the same material properties which young's modulus and Poisson's ratio are housed as 2.0E+05MPa and 0.3 respectively.

3.4 Mesh Generation

Mesh generation is one of the most important parts in finite element analysis. Defining smooth regular elements and connecting elements by appropriate elements types is a common method to build up a good quality mesh model. Errors can be avoided in further calculations when a good quality mesh model is used to assemble element matrix. Various meshing tools are available in ANSYS software.

To generate the suitable mesh for a gusseted k joint including the diagonal , bottom chord and welding segment connecting them, neither pure tetrahedral element nor pure quadrilateral elements meshing is appropriate. Using the meshing tool provided by ANSYS, tetrahedral element was created in both gusset plate and other member of k joint. There are very versatile options are available for meshing i.e. line mesh, area mesh, volume mesh, smart size, manual size, concentrate meshing etc. Refining the mesh on certain area of the model can make nice additional contribution to the model which is available in ANSYS.

3.5 Loading and Boundary Condition

3.5.1 For the 3D Bridge Analysis

For the 3D analysis of bridge the applied boundary condition is hinged connection at one end and roller connection at other end. IRC CLASS-A loading is applied for the linear analysis of bridge. The analysis is carried out only moving load case. The frame elements were used for modeling the bottom chord and diagonal members in 3D finite element model of bridge.

3.5.2 For the k - Joint

The boundary condition for k-joint was applied after studying the various past literatures. There are very few literatures available in this topic. The researchers G.J Van Der Vegte, et.al (2004) Kumamoto University, Japan/Delft University of Technology had studied the Influence of boundary condition on the chord load effect for the CHS Gap k- joints. They studied the influence of boundary condition on different four cases and find the best boundary condition. In this research the boundary condition was taken from above researcher's conclusion.

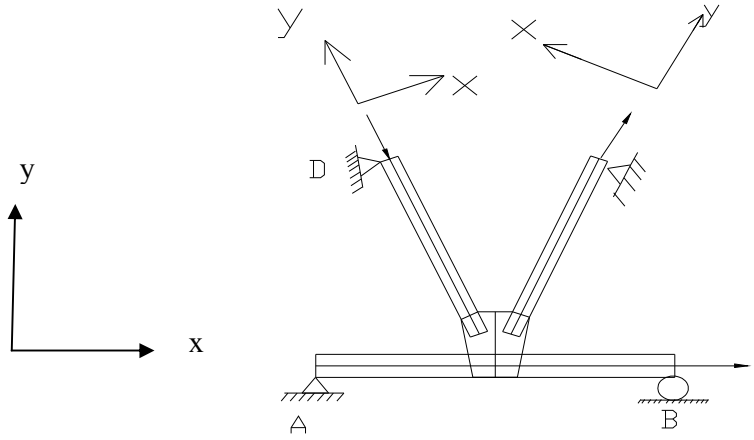

Figure 3.2: Applied Boundary Condition.

Applied Boundary Condition

Degree of freedom	Node on A	Node on B	Node on C	Node on D
U_x	0	Free	0	0
U_y	0	0	free	free
U_z	0	0	0	0

The load was applied at right end B and diagonal member end C and D as a pressure load per unit area.

4. NUMERICAL ANALYSIS

4.1 3D Analysis of Bridge

All calculations are performed on pc using the software package SAP2000 (Ver.10.0.1). Using the frame element 3D FE model of 50 m bridge was created .At first all the section property of the bridge members were find out using section builders in SAP. Then all the properties are assigning in FE model. Using the Bridge Wizard menu of software, lane width 3.5m and IRC –Class A loading was applied. After applying the boundary condition and material properties the model was run for linear analysis. The ultimate objective in carrying out linear analysis is to find out the force and displacement. In this study the critical joint was found out by comparing the axial force value and joint displacement only. The output of analysis i.e. shear force, bending moment and torsion are the beyond the scope of this work. The result obtained from analysis is presented in chapter five.

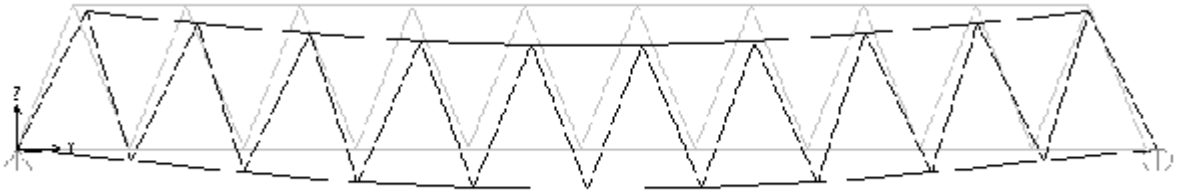

Figure 4.1 Deformed shape of bridge in XZ plane

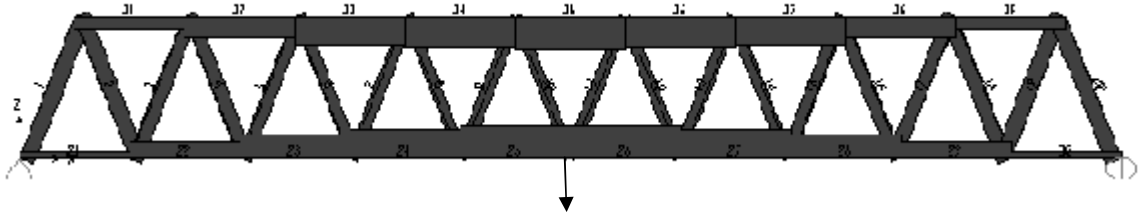

Maximum displacement and force joint: See result in chapter five

Figure 4.2 Axial force of bridge in IRC class –A loading

4.2 Modeling and Analysis of K- Joint and

All calculations are performed on pc using the software package ANSYS (Ver.10).3D FE model of k - joint was created. The ultimate aim of this research work is to find out the fatigue damage of welded joint.

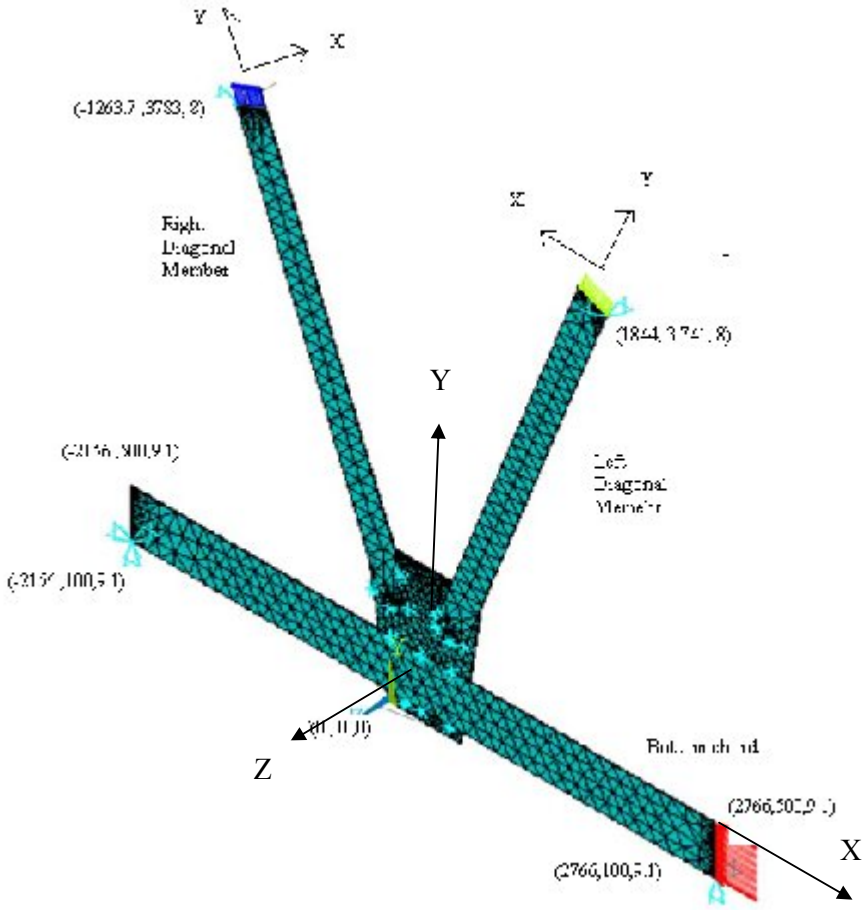

Figure 4.3 Finite element model of k joint

The 3D FE model was created using the element mention in chapter 3, finite element model. The three different models using the different weld radius, 2mm, 3mm and 5mm were created using the preprocessor menu in ANSYS. Model contains the twenty two thousand one hundred four nodes and nine thousand nine hundred thirty two elements.

The axial load was applied obtained from the analysis of bridge from the solution

menu. As mention below:

Solution

Analysis Type

New analysis

Transient – ok.

Solution control

Basic tab

Time at the end of load step= 10 second.

Transient tab

Steeped loading - ok

Define loads

Apply /structural displacement/area/select all area

Displacement = 0 ok.

Force/moment / pressure

Pick area 1BC / direction along - F_x

Pressure = 204N/mm^2

Pick area 2 DM / direction along – Fy (local coordinate system)

Right DM = +84N/Mmm^2

Left DM = - 84N/mm^2

Load step opts

Write LS file

Load step file number n = 1 ok.

Analysis Type

Solution control

Basic tab

Time at the end of load step= 20 second.

Transient tab

Steeped loading - ok

Delete load

Delete /structural/force/moment/pressure

Select all area – ok

Apply

Structural

Force/moment / pressure

Pick area 1BC / direction along - F_x

Pressure = 204N/mm^2

Pick area 2 DM / direction along – Fy (local coordinate system)

Right DM = -84N/Mmm^2

Left DM = +84N/mm^2

Load step opts

Write LS file

Load step file number n = 2 ok

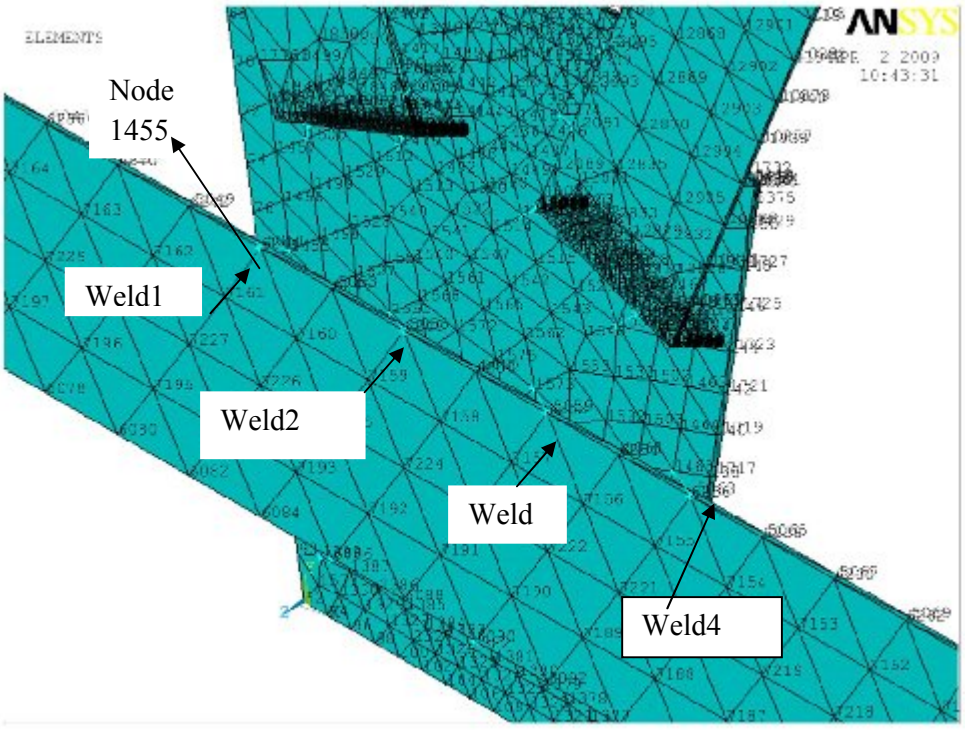

Figure 4.4: FE model showing welding location

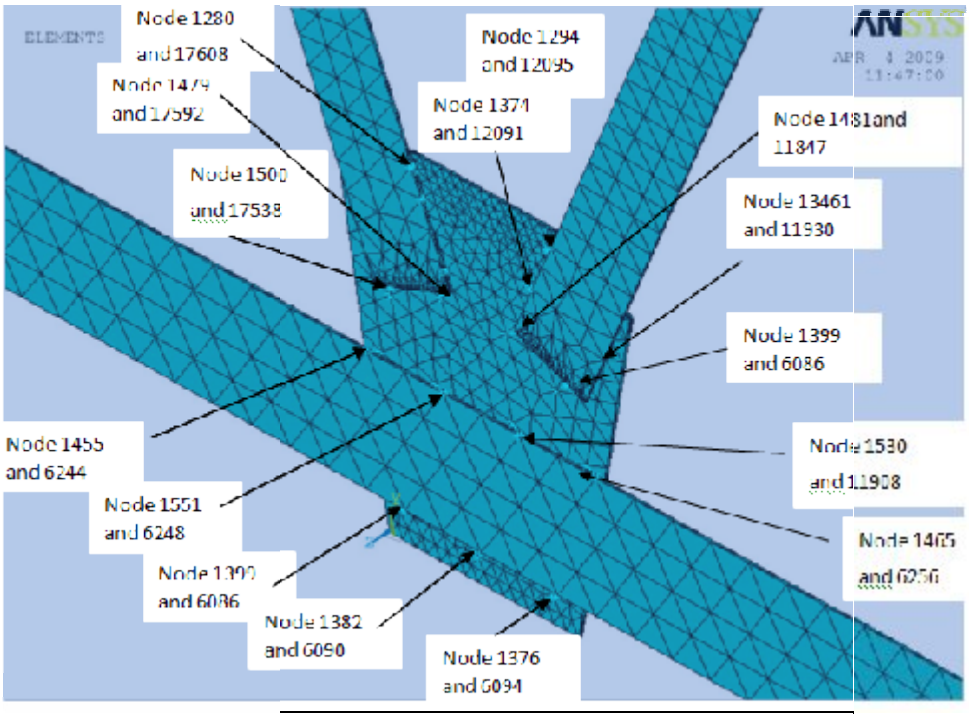

Figure 4.5: Node number of Welded connection

There are several FEA based methods for obtaining the stress information that is required to perform a fatigue life calculation. But in this search work Transient No-linear elastic perfectly plastic analysis were carried out which widely used method for fatigue calculation. If this approaches is used the stress histories are produced at each point of interest. These stress histories are also superimposed to obtain the required combined stress histories, but FE solver handles this. Fatigue life calculations are then performed on these stress time histories.

4.3 Evaluating Fatigue

The ANSYS fatigue calculation rely on the ASME boiler and pressure vessel code, section III for guidelines on range counting ,simplified elastic plastic adaptations, and fatigue summation by miner's rule. The following are the step followed to calculate the fatigue damage in ANSYS.

1. Enter POST1 and resume database.

   The result obtained from the analysis of joint was stored at preselected locations. All the stress result for welded node was resumed.

2. Establish the size, fatigue material properties(S-N), and location.

   By default, Ansys fatigue evaluation can consider up to five nodal locations, ten events, and three loading within event. In order to calculate the usage factors, and the effect of simplified elastic-plastic computations, material fatigue properties S-N curve was kept using IS code and considering the F-class constructions details as shown in Annex F.

3. Store stress and assign event repetition and scale factors.

   In order to perform a fatigue evaluation, the program must know the stresses at different events and loadings or each location, as well as the number of each event.

4. Activate the fatigue calculations
5. Review the result
6. Repeat same procedure for various locations.

5. RESULT AND DISCUSSION

5.1General

Finite element analysis as a numerical method provides a way to simulate and analyze actual structures. The nodal result obtained from a FE method is approximated element by element, in a piecewise fashion. Although the structural displacement derived from the nodal results of finite element analysis are not 100% precise, they can provide an accurate solution in the level defined by researchers. The primary unknowns calculated in a structural analysis are displacements. Other quantities, such as strains, stresses, and reaction forces, are then derived from the nodal displacements are required .All the result of the structural members and structural connections were derived from the program. The maximum strain, stress and displacement were observed and areas were presented herein.

5.2 3D Analysis of Bridge

The critical study of numerical analysis reveals some important findings. The result obtained from the linear analysis of 3D bridge is presented here though this is not the main aim of research. In case of moving load the influence line diagram is very important for various structural quantities. According to the position of load the value of structural quantities varies. It is necessary to find the position of load that gives the maximum value of stress, strain and displacements. In this research work position of load for maximum structural quantities was found and applied in FE model. The result obtained from the analysis clearly shows that why the middle joint was taken for fatigue calculation.

Main focus was made on only axial force and displacement of various member and joint. The result obtained from the analysis is presented here in graphical form so that we can compare easily.

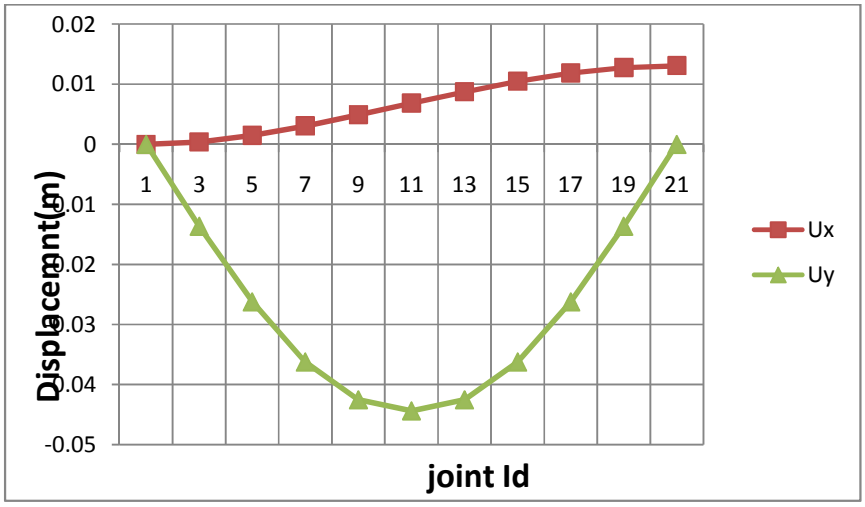

Figure 5.1 Displacement along x and y direction of 3D Bridge

From the figure 5.1 it is clear that the displacement along the longitudinal direction (x-direction) is increasing from left to right. The support condition of left end is displacement along x and y direction is restricted but in case of right end only displacement along y -direction is restricted. The displacement along the x-direction increases rapidly up to the joint 11 and increases slightly then after. Displacement in y- direction is maximum in joint 11. The displacement in y-direction is increases up to joint 11 then decreases. Vertical displacement in joint 11 is 44.381 mms that is maximum m in the span

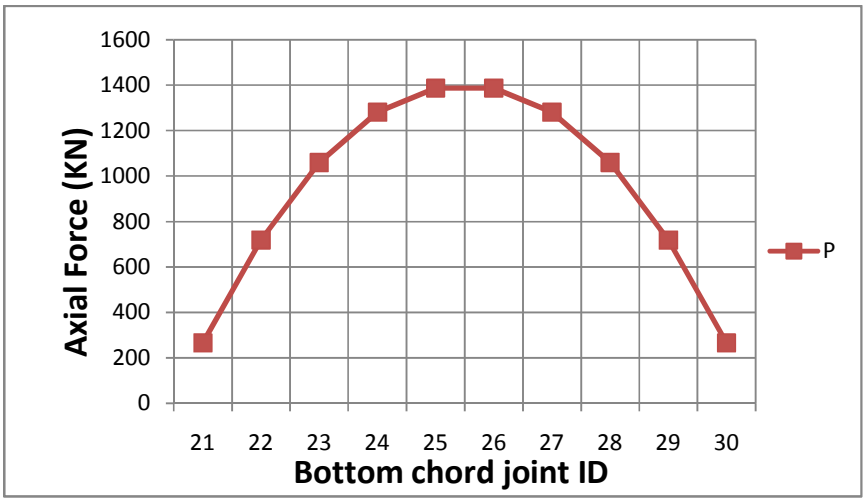

Figure 5.2 Bottom Chord Members Axial Force of 3D Bridge

The Analysis shows that axial force in bottom chord is always tension and its value is maximum in the middle part of bridge span. The bottom member ID 25 and 26 have maximum axial force of 1386.522KN. The result shows that the strength of bottom chord member should not be kept same throughout the span of bridge. The section provided in mid span should have sufficient to strength and connection should be safe for that load.

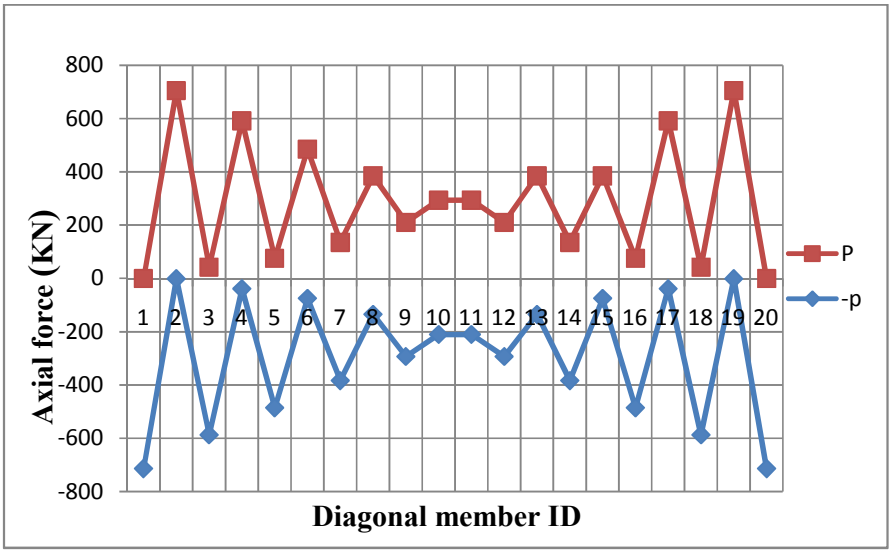

Figure 5.3 Axial Forces in Diagonal Member of 3D Bridge

Figure 5.3 clearly shows that the diagonal member of truss bridge experiences both tensile and compressive forces. The diagonal member corresponding to the maximum axial force is 10 and 11 as shown in figure 5.3. Diagonal member 10 have to resist the positive axial force 294.057 KN and negative axial force 209.822KN.similarly, diagonal member 11 have to resist the positive axial force 294.088 KN and negative axial force 209.82 KN. This shows that diagonal member should be checked with dynamic loading fatigue design criteria. When subjected to repetitive loading during service life even if the dynamic stresses are modest and well below the yield limit fatigue damage may occur.

Ultimately the load from the diagonal member and other chord should transfer from the joint. In case of weld connection weld also experience the dynamic force but we

know weld is very weak in dynamic loading. Various failure mechanisms have to avoid through appropriate design, choice of material and structural dimension. It is however fact that welded joints are particularly vulnerable to fatigue damage when subjected to repetitive loading.

5.3 Analysis of Welded k- Joint

Various parametric investigations are made to compare the result of different weld radius, 2mm, 3mm and 5mm. The solution can be extracted for ten second and twenty. The main aim is to focus the nature of joint in dynamic loading so all the graph present here are for ten second. For the calculations of fatigue both ten second and twenty second stress was used. The result for twenty second is kept in annex C.

5.3.1 Effect of Weld Radius on Displacement

Comparing the result the analysis shows that displacement along the longitudinal direction (x- direction) is decrease with the increased of weld radius. In case of weld radius 2mm the displacement in x direction is 86 mm but in case of weld radius 5mm the displacement in longitudinal direction is 77.768 mm which is almost 11% less than 2mm weld radius. The tabulated data are kept in Annex.

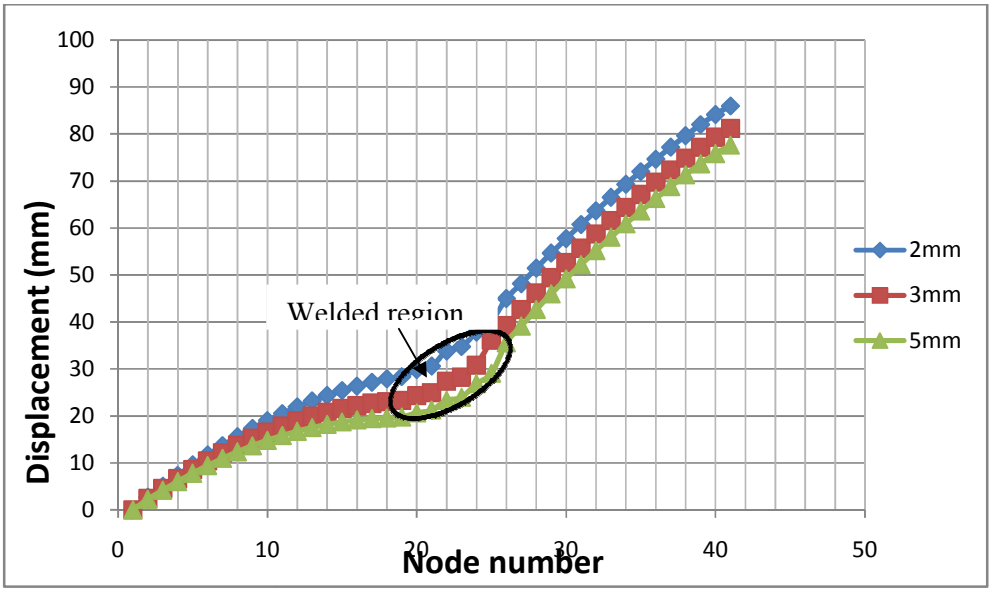

Figure 5.4 Displacement in x –Direction of K- joint

From the figure 5.4 and the figure 5.1 we can compare the nature of the longitudinal displacement. The displacement in the joint in case of 3D bridge analysis was 6.855mm whereas the displacement in the k joint model was 27.90mm, 23.047mm and 19.556mm respectively in the weld radius 2mm, 3mm and 5mm.The difference in displacement may be due to the effect of material non linearity in k- joint model and not in 3D bridge. However if we consider the material non linearity in both cases then the result may be almost same.

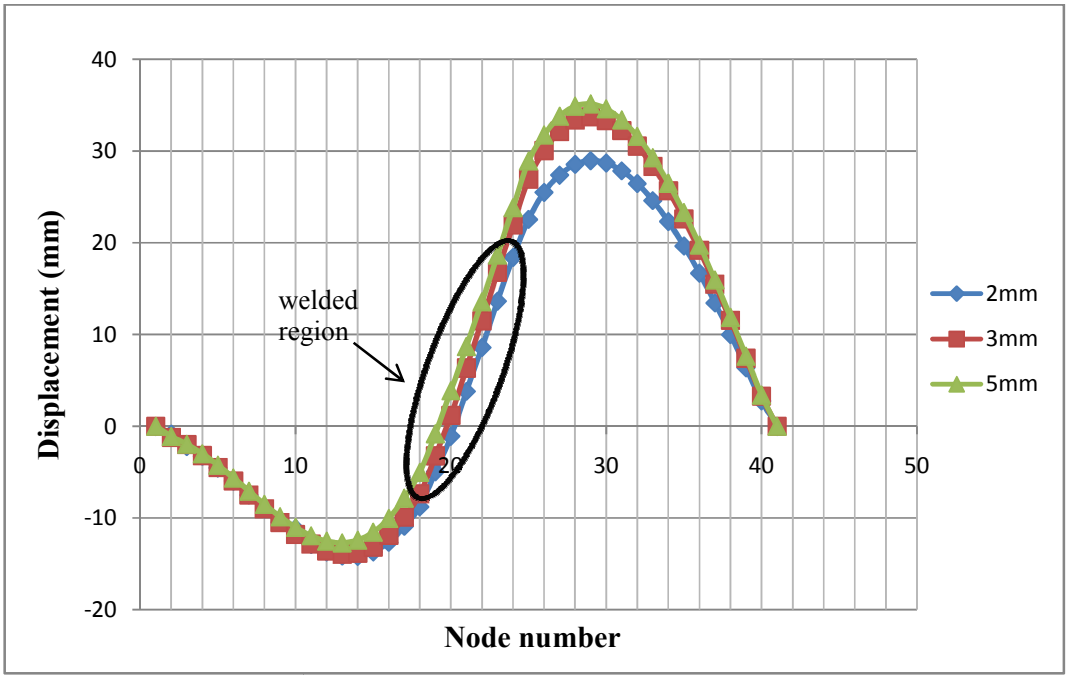

Figure 5.5 Displacement in y- Direction of K-joint

Weld radius has effect on displacement in y – direction. Comparing the result there is slightly higher value of displacement in weld radius 5mm than the weld radius 2mm.This may be due to the higher load carrying capacity of weld with increase of weld radius. Maximum value of positive displacement in case of weld radius 2mm is 29 mm and in case of weld radius 5mm is 35.134mm.The displacement values are both positive and negative. The displacement in y- direction in the section right of gusset plate is upward but in case of right of gusset plate the displacement in y-direction is negative. From the result we can say that end welded node should experience maximum strain that is why chance to failure from end weld.

5.3.2 Effect of Weld Radius on Stress

In order to find out the effect of weld radius, stress distribution need to be investigated. The node stress value delivered a good representation of stress distribution. The main focus was given to study the normal stress, shear stress and von misses stress on weld. To check the weld capacity shear stress is very useful. Von misses stress gives the most meaningful stress map under the given loading. Von misses stress is used to estimate yield criteria for ductile material. The analysis shows that the nature of stress distribution in bottom chord, diagonal chord and gusset plate is different. So discussion on the result are presented here

Bottom Chord Welded Node

The bottom chord is attached with gusset plate by welding on top and bottom as shown in figure 4.5. Stress on top weld and bottom weld may be different. Stress on chord and gusset plate is also different. Normal stress is decreased with the increases of weld radius. In figure 5.6 the node 1 represent the first weld point 1455 of bottom chord and the 4th node represent the node 1465. Node 1 has lower value of normal stress than the other node. 4th node is near to the application of load than the other node. From this result we can say that end weld experiences maximum normal stress. With the increase of weld radius normal stress decreases. Normal stress in 5mm weld was up to 100% less with 2mm weld and 33% with the 3 mm weld.

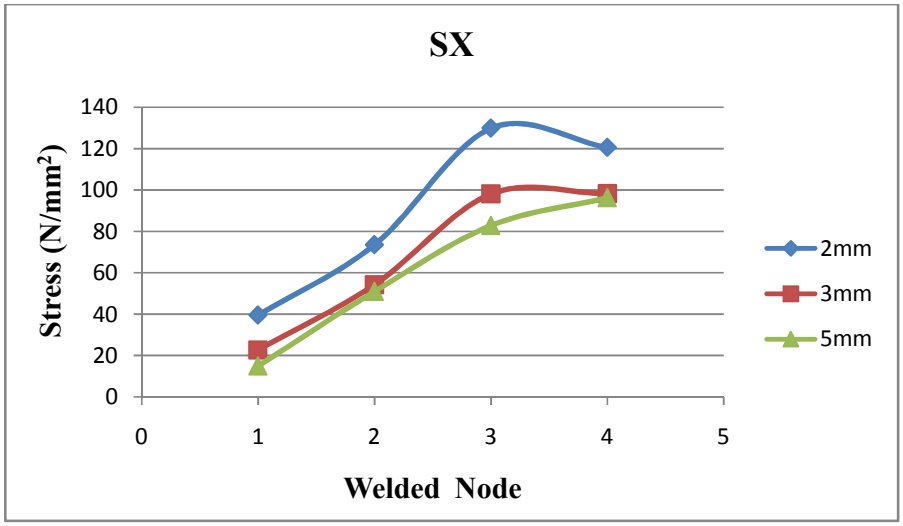

Figure 5.6 Normal stress Sx in Bottom chord welded node 1455

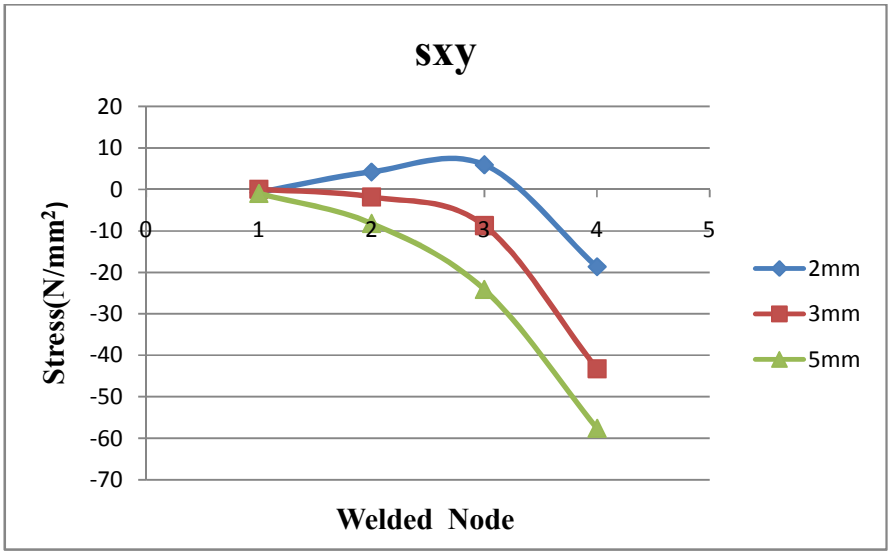

Figure 5.7 Shear stress Sxy in bottom chord welded node

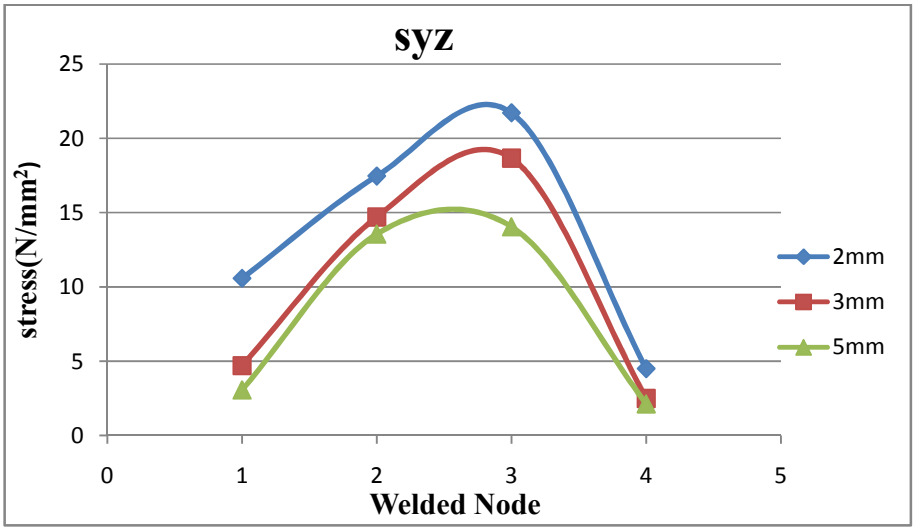

Figure 5.8 Shear Stress Syz in bottom chord welded node

Shear stress Sxy and S_{yz} also decreases with the increases of weld radius. Shear stress S_{xy} is both positive and negative value where as shear stress Syz is only positive value. From the figure 5.7 we can see that shear stress is minimum in node 1455 and maximum in node 1465. Node 1455 is far from the loading edge so shear stress value also very low. Shear stress in yz direction is maximum in middle welding node as shown in figure 5.8. From above shear stress diagram, analysis shows that weld

experience dynamic forces so welded joint should full fill the requirement of fatigue design.

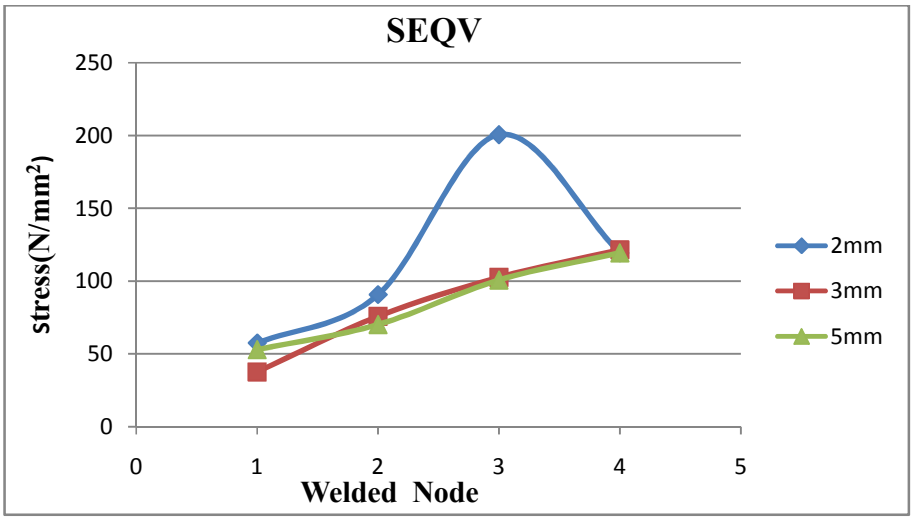

Figure 5.9 Von-Misses stress on welded point

The distribution of von-misses stress is non uniform in case of weld radius 2mm. Some point offers very high stress and other with low stress. But if we increase the weld radius, analysis shows that the distribution of stress is almost uniform. Generally from figure 5.9 we can say that von-misses stress is decreased with the increased of weld radius. Refer table A.C.1 and table A.C.2.

Gusset Plate Welded Node

Analysis shows that increase in weld radius decrease the displacement on longitudinal direction. It is interesting to find out that the effect of weld radius on gusset plate by observing the stress on different weld radius and comparing the result. The normal stress S_x in gusset plate is both compressive and tensile nature but in case of bottom chord it is tensile nature. From the 5.10 the gusseted welded node experiences both tensile and compressive normal stress. When the vehicles moves from left to right the some of the welded node experiences tensile stress and other compressive forces. If the direction of vehicles is vice right to left direction then stress also vice versa.

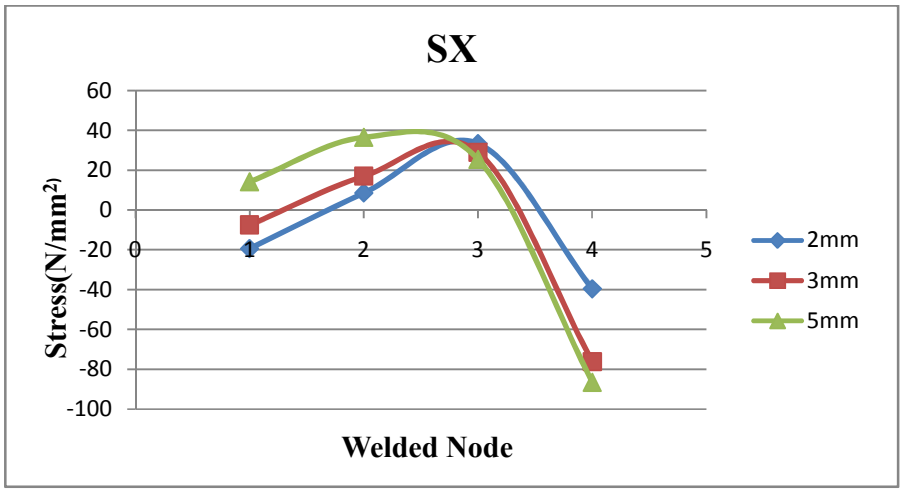

Figure 5.10 Normal stress Sx on gusset plate welded node

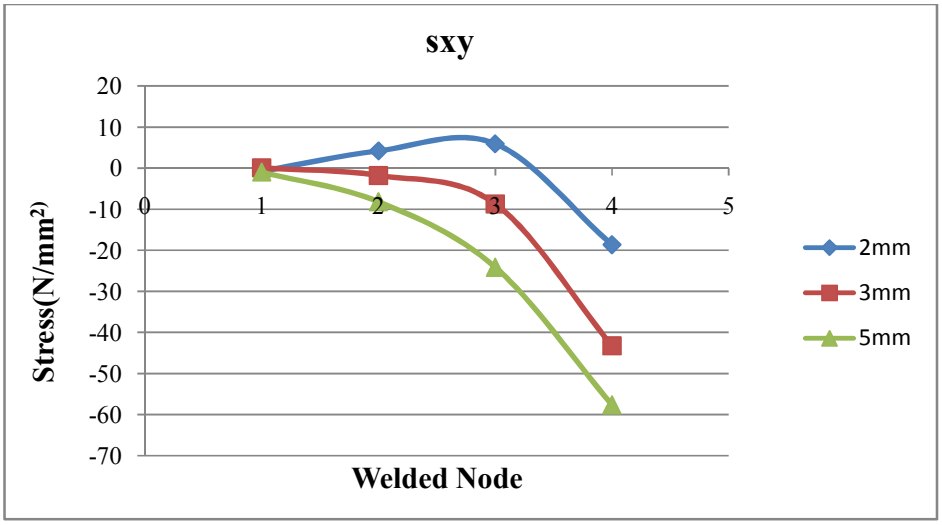

Figure 5.11 shear stress Sxy on gusset plate welded node

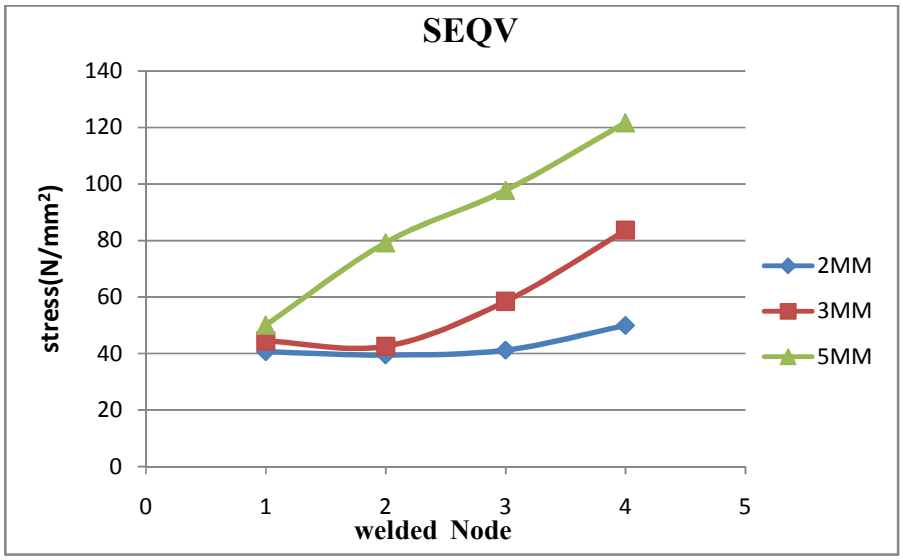

Figure 5.12 Von- misses stress SEQV on gusset plate welded node

The shear stress in gusset plate is the same magnitude of bottom chord welded node. The analysis shows the really interesting result on gusset plate and bottom chord welded node. In case of bottom chord if we increased the weld radius the von misses stress decreased but it is increase in gusset plate. So if we increased the weld radius we must take care about the thickness of gusset plate also it may buckle. The stress in gusset plate is increases from left node to right node of gusset plate.

Diagonal Member: Left Diagonal Member

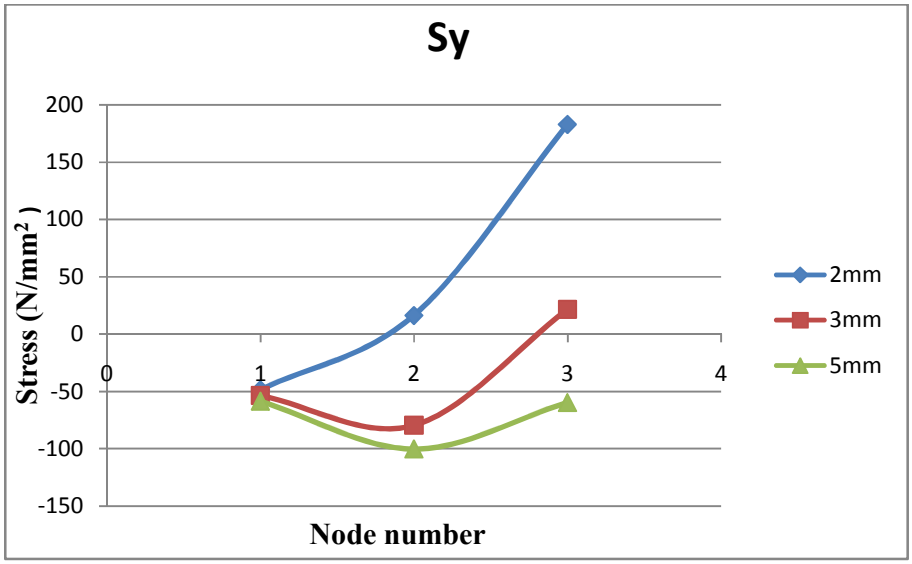

Figure 5.13: Normal stress on right diagonal member on node 17608, 17606 &19705

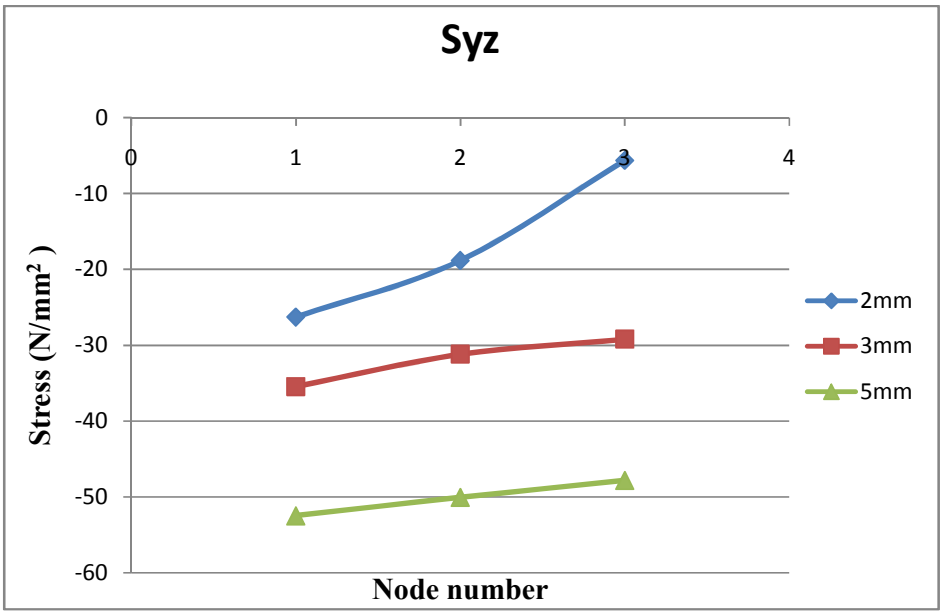

Figure 5.14: Shear stress on right diagonal member on node 17608, 17606 &19705

5.3.3 Effect of Weld Radius on Fatigue Damage

The mechanical features are important aspects of welding process since they have great influences on the properties of the welded joint and the quality of the welded structure such as the failure strength, fatigue and so, on. In this research work, a finite element analysis was conducted to simulate the mechanical behavior of the welding process. A FE model was developed using the software ANSYS .The stress and strain distributions in the welded node were determined. The transient non- linear analysis was performed to determine the stress and strain result from the finite element model. The results of the maximum principal stresses and strain are used for the subsequent fatigue life analysis.

The S-N curves for welded joints have just one key parameter to the fatigue life. In this research work for the calculation of fatigue damage the S-N curve was taken as a class F construction detail from IS1024.If some of the stress variation is partially in the compressive side, this will not contribute to the fatigue damage to the same extent as variation on the tensile side. In this research work fatigue damage calculation was done only in the welded node because all the past literatures clearly mention that these are vulnerable to fatigue. The fatigue damage calculation was done by comparing the applied number of cycles n_i at a given stress level with the experimental number of cycles to failure N_{Ti}.

Fatigue damage is calculated almost all the welded node on the joint. Fatigue damage is calculated on gusset plate, bottom chord, and diagonal members welded node. Fatigue damage is calculated on three different 2mm, 3mm and 5mm weld radiuses on same joint. In the same alternating stress various numbers of cycles was applied and fatigue damage was found out.

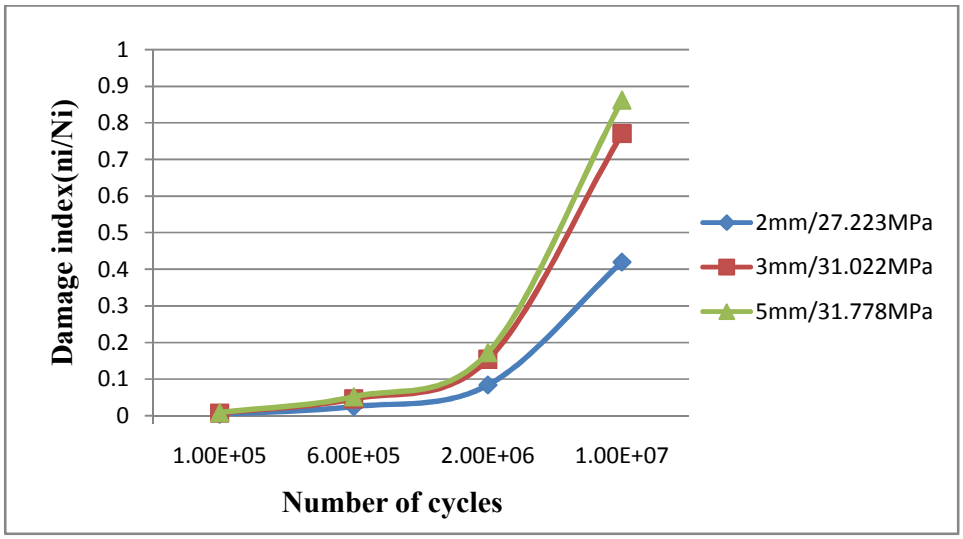

Figure 5.15: Fatigue damage in bottom chord welded node 1455 with different weld radius and different alt. stress

From the figure 5.13 we can say that same weld node 1455 experiences different alternating stress with different weld radius. In case of weld radius 2mm the alternating stress was 27.223MPa and corresponding fatigue damage in different cycles are show in figure and tabular form in annex. The number of cycles required to failure the welded node 1455 at alt.stress level 27.223MPa was 2.38E+07 cycles. The number of cycles required to failure the same node in case of 3mm weld radius is 1.30E+07cycles at alt. stress 31.022MPa.Similarly number of cycles required to failure the same node in case of 5mm weld is 1.16E+07 cycles at alt. stress level 31.778MPa.

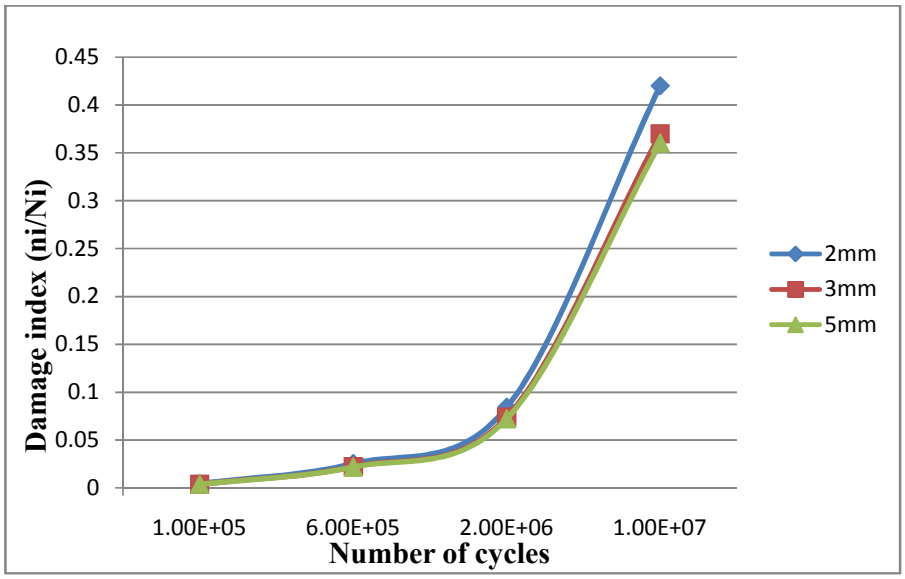

Figure 5.16: Fatigue damage in bottom chord welded node 1455 at alt. Stress 27.223MPa

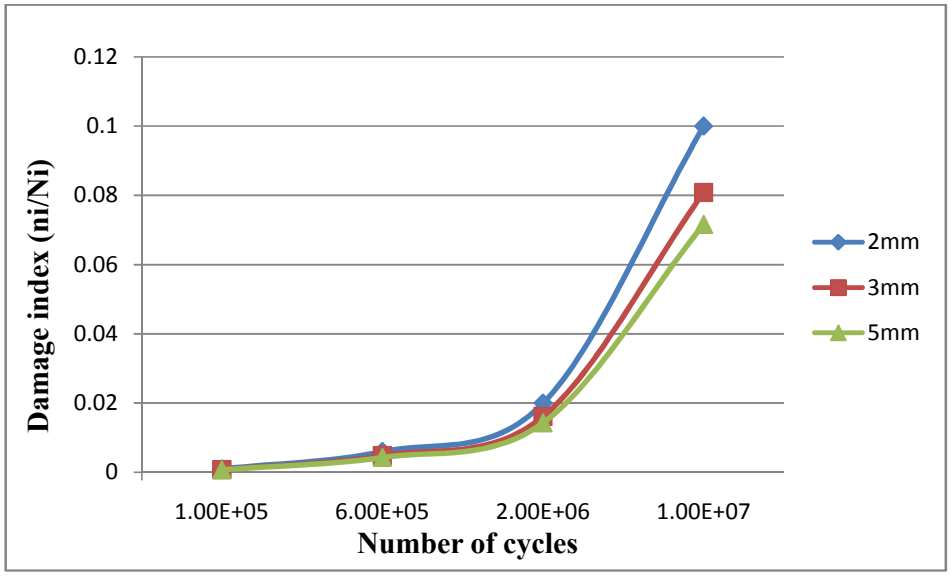

Figure 5.17: Fatigue damage in Gusset plate welded node 6244 (1455 and 6244 are welded node) at alt. Stress 10.318 MPa

.

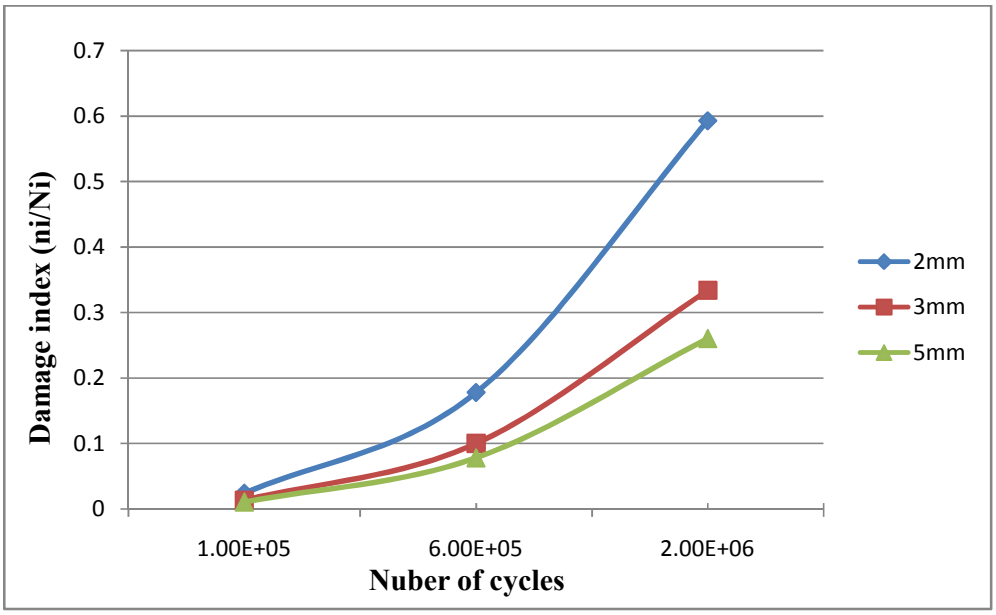

Figure 5.18: Fatigue damage in diagonal member welded node 1481 at alt. Stress 41.392 MPa

From the figure 5.16 and figure 5.17 it is clear that at the same stress level the fatigue damage is decreased with increased of weld radius. The analysis shows that fatigue damage in bottom chord is more than the gusset plate. In case of 5 mm weld the fatigue damage in 1.00E+07cycles in bottom chord is 0.360 and gusset plate is o.071. Probability of failure of welded joint is greater in bottom chord welded node then the gusset plate welded node. The fatigue damage is in bottom chord was 14.28% less in 5mm weld radius with compares to 2mm weld radius. Similarly fatigue damage in gusset plate was 29% less in 5mm weld radius with compares to 2mm weld. The analysis shows that weld radius less than 3mm should not be provided.

Comparing the result of diagonal member and bottom chord the fatigue damage in case of 5mm weld in bottom chord at 2.00E+06 number of cycles is 0.072 .But this value is 0.2603 in diagonal member in 5mm weld radius and 2.00E+06 number of cycles. From here it is clear that diagonal member's welded nodes are more vulnerable in fatigue loading. Diagonal member experiences higher value of alternating stress than the bottom chord. However the axial force was more in bottom chord than in diagonal member.

6. CONCLUSIONS

The main goal of this research work was to develop a FE model representing the welding and calculating the fatigue damage on welded node. The focus of this fatigue capability was gain insight into the current life predication methodologies and their use. A critical issue facing by engineers is effect of dynamic load in case of welded joint. Therefore it was demonstrated that available software can be used to calculate the fatigue damage.

In case of this research size of weld used in Rapti Bridge was not known so different weld radius was used for FE model and fatigue calculation. The analysis shows that stress concentration around the weld is more than the other point. There are various uncertainties in different welded part of bridge. That is why we cannot say this bridge will fail or not by fatigue. The welds are usually not included in the FE model, which cannot represent the real behavior of welded joint. In this research work welded joint are simulate in FE model and the boundary condition was applied from the previous literature study.

The present research is to address the two major issues; first the effect of weld radius on fatigue damage and second effect of weld radius on stress and strain behavior of joint. The whole of the effort is expended in this research to make a FE model representing the welding. Number of parametric studies is made to gain the confidence in result. The following list summarizes the primary conclusion regarding the behavior and fatigue damage calculation of welded k- joint.

1. The linear analysis of 3d bridges shows that the entire bottom chord member experiences the tensile force, top chord experiences the compressive forces and diagonal member experiences both tensile and compressive forces. That is why for the design of welded joint fatigue criteria should be checked.

2. The analysis shows that increase in weld radius decrease the displacement along the x- axis. The displacement along the x- axis respectively in case of

2mm, 3mm, and 5mm weld radius are 86mm, 81.172mm, and 77.682 mm

3. The distribution of stresses is more uniform in 5mm weld radius than 2mm weld radius. In case of low weld radius there is very high fluctuation of stress in nearby point.

4. By increasing the weld radius we can decrease the value of alternating stress. But some point shows the high value which may be the stress concentration around that point. The value of alternating stress at node 1455 having different weld radius 2mm,3mm,5mm is respectively 41.392MPa, 37.398MPa,35.453MPa.

5. The analysis shows that the load on gusseted k-joint does not only transfer from the diagonal brace to chord. But also from the diagonal member to the gusset plate and eventually to the chord. So gusset plate should be designed to resisting such forces. IS code does not mention the design criteria about the gusset plate. From the result of this study it is clear that the gusset plate need to be design.

6. Increase in weld radius decreased the fatigue damage. The fatigue damage is less in gusset plate node than the chord node.

7. IS codes does not limit the size of weld for the dynamic loading. But minimum size of weld restricted by the code, indirectly limits the minimum weld size for repetitive loading. The weld radius less than 3mm should not be provided in repetitive loading.

8. The analysis shows that the diagonal member's welded connection is more vulnerable in dynamic loading.

7. RECOMMENDTAION

Future work needs to perform in several key areas. These could not be realized in this research work due to the limitations of time, knowledge and resources. The recommendations for the future works are summarized under

1. The analysis can be extended for modeling of weld giving input, voltage, current, welding speed, welding diameter etc.

2. The model can be run for different boundary condition which gives the best result.

3. S-N method does not give information about the crack initiation and propagation. To calculate the fatigue damage Linear Elastic Fracture Mechanics can be applied.

4. The analysis can be extended using other Non-linear constitutive laws.

5. The analysis can be extended towards preparing the model representing the effect of weld imperfections i.e. undercut, slag line, lack of fusion, porosity, misalignment etc.

REFERENCES

1. Alam, M.S. and Wahab, M.A. (2005). "Modeling of Fatigue Crack Growth and Propagation Life of Joint of Two Elastic Materials Using Interface Elements. International Journal of Pressure Vessel and Piping, 82, pp. 105-113.
2. Ahmet Hanifi ERTAS and Fazil Onder SONMEZ (2007). "A Parametric Study on Fatigue Life Behavior of Spot Welded Joints." Proceedings of the 8th International Conferences.
3. Alam, M.S. and Wahab, M.A. (2005). "Modeling of Fatigue Crack Growth and Propagation Life of Joint of Two Elastic Materials Using Interface Elements." International Journal of Pressure Vessel and Piping, 82, pp. 105-113.
4. ANSYS, INC., Modeling Software, ANSYS 10.0 Documentation, 2004
5. Andrea Carpinteri. (1994). "Handbook of Fatigue Crack Propagation in Metallic Structures." ELSEVIER SCIENCE B.V
6. Bell, R., and Vosikovsky, o. (1992). "A Fatigue Life Prediction Model for Multiple Cracks in Welded Joints for Offshore Structures." OMAE, Vol. III-B Material E\ngineering, ASME.
7. Baharam Farahmand, Ph.D, Boeing Technical Fellow (2001) "Fracture Mechanics of Metals, Components, Welds, and Bolted Joints." Kluwer Academic Publication
8. Barsom, J. M., (1994). "Fracture Mechanics Analysis of Fatigue Crack Initiation and Growth." The International Conference on Fatigue, Toronto, Ontario Canada, 88-98
9. Chandra, Ram (2002). "Design of Steel Structures." Standard Book House
10. Elber, W. (1970). "Fatigue Crack Growth under Cyclic Tension." Engineering Fracture Mechanics, 2, pp. 37-45.
11. Erdogan Madenci and Ibrahim Guven (2006). The Finite Element Method and Application in Engineering Using ANSYS.

12. Ferrica, J.A and Branco, C.M. (1990). "Fatigue Analysis and Prediction in Fillet Welded Joints in the Low Thickness Range." Journal of Fatigue & Fracture of Engineering Materials and Structures, Vol.13,No.3,PP.201-212.

13. Gang, Zhao (2006). "Finite Element Analysis and design of welded HSS connection." North Carolina State University.

14. Glinka, G. (1994). "Fatigue Crack Growth and Effects of Residual Stresses" The International Conference on Fatigue, Toronto, Ontario Canada, pp. 99-123.

15. Gurney, T.R. (1979). "Fatigue of Welded Structures." 2nd Edition, Cambridge University Press, London.

16. Howard, E. Boyer (1986)."Atlas of Fatigue Curves." American Society For Metals."

17. Hobbacher, A (1996). "Fatigue Design of Welded Joints and Components." Abington Publishing.

18. Kanninen, F. Melvin and Popular, H. Cari (1985). "Advanced Fracture Mechanics." Oxford Engineering Science Series 15, Oxford University Press.

19. Lassen, Tom and Recho, Naman (2007). "Fatigue Life Analysis of Welded structures." First South Asian Edition

20. Lindgren, L. E. (2001). "Finite Element Modeling and Simulation of Welding Part 1: Increased Complexity." Journal of Thermal Stress, 24, 141-192.

21. Linda, R. (1990). "Fatigue Crack Growth of Weldments. Fatigue Fracture Testing of Weldments, ASTM Publ.STP 1058,pp 16-33.

22. Madayag, A. F. "Metal Fatigue: Theory and Design, Wiley. "New York, 1969.

23. Maddox, S.J. (1993). "Recent Advances in the Fatigue Assessment of Weld Imperfections." Welding Journal, 72 (7), pp. 42-52.

24. Maddox, S.J. (1974). "Fatigue Crack Propagation Data Obtained From Parent Plate, Weld Metal and HAZ in Structural Steels." WRI, 4(1), pp. 32-42.

25. Murthy, R.D.S., Gandhi, P. and Rao, Madhava A.G. (1994). "A Model for Fatigue Prediction of Offshore Welded Stiffened Steel Tubular Joints Using FEM Approach. International Journal of Offshore and Polar Engineering.

26. Newman, J.C. Jr. (1977). "Finite-Element Analysis of Crack Growth under Monotonic and Cyclic Loading." ASTM STP 637, Philadelphia, PA, 56-80

27. Paris, P., and Erdogan, F. (1963). "A Critical Analysis of Crack Propagation Law." J. of Basic Engineering, Vol. 85, pp. 528-534.

28. Rahaman, M.M, Baker, A.Rosil, Rejab, M.R.M and Sani, M.S.M. (2008). "Fatigue Life Prediction of Spot-Welded Structures: A Finite Element Analysis Approach."European Journal of Scientific Research. http://www.eurojournals.com/ejsr.htm

29. Sanders, W.W. Jr. and Lawrence F.V, Jr. (1977). "Fatigue Behavior of Aluminum Alloy Weldments." Fatigue Testing of Weldments, ASTMSTP 648

30. Verma, Dhirendra (1996). "Fatigue Crack Growth," Published by New Age International (p) Limited.

31. Vander Vegte, G.J, Makino, Y. and War denier, J. (2004). "The Influence of Boundary Condition on the Chord Load Effects for CHS Gap K- Joints." Connection in Steel Structures V –Amsterdam-June 3-4, 2004.

32. Wu, W. (2002) MS Thesis. "Department of Mechanical Engineering, University of New South Wales, Australia."

.

.

APPENDICES

APPENDIX A

OUTPUT FOR 3D ANALYSIS OF BRIDGE: SAP2000

Section Property Data

Table A.A.1: Section Property Data of 3D Bridge

section Property	Bottom Chord BC-1	Bottom Chord BC-2	Bottom Chord BC-3	Cross Beam Assembly	Stringer Beam Assembly
A	0.016	0.016	0.0168	0.0293	0.014
J	6.804 E-04	6.804 E-04	7.15E-04	5.42E-04	1.02E-04
I33	4.50E-04	4.50E-04	4.75E-04	1.47E-03	3.42E-04
I22	5.24E-04	5.24E-04	5.28E-04	1.86E-04	3.07E-04
I23	0	0	0	0	0
AS2	7.23E-03	7.23E-03	7.28E-03	0.0202	9.59E-03
AS3	7.37E-03	7.37E-03	8.23E-03	0.0119	6.36E-03
S33(+face)	2.18E-03	2.18E-03	2.36E-03	4.11E-03	1.39E-03
S33(-face)	2.18E-03	2.18E-03	2.22E-03	4.58E-03	1.49E-03
s22(+face)	2.35E-03	2.35E-03	2.37E-03	1.60E-03	4.77E-04
s22(-face)	2.35E-03	2.35E-03	2.37E-03	1.60E-03	4.77E-04
z33	2.51E-03	2.51E-03	2.63E-03	5.87E-03	1.96E-03
z22	2.745E- 3	2.745E-0.3	2.79E-03	1.91E-03	5.84E-04
r33	0.1666	0.1666	0.1681	0.2238	0.1563
r22	0.1797	0.1797	0.1772	0.0797	0.01563
xcg	2.83E-18	2.83E-18	2.73E-18	-4.43E-19	-6.79E-19
ycg	-2.45E-18	-2.45E-18	7.42E-03	0.0206	0.0302
Xpna	0	0	9.26E-03	7.15E-03	0.0121
Ypna	0	0	0	0	0

Table A.A.2: Section Property Data of 3D Bridge

section Property	Top Chord TC-1	Top Chord TC-2	Top Chord TC-3	Diagonal Member A/B	Diagonal Member C1	Diagonal Member C2	Diagonal Member C3/C4
A	0.0155	0.0161	0.0167	0.0138	0.0115	0.0127	0.0115
J	4.56E-04	4.80E-04	5.04E-04	3.21E-04	2.16E-04	2.83E-04	2.52E-04
I_{33}	2.24E-04	2.38E-03	2.51E-04	1.92E-04	1.86E-04	1.39E-04	1.19E-04
I_{22}	4.85E-04	4.90E-04	4.44E-04	4.57E-04	3.61E-04	3.70E-04	3.61E-04
I_{23}	0	0	0	0	0	0	0
A_{S2}	8.18E-03	8.22E-03	8.28E-03	7.79E-03	5.51E-03	5.62E-03	5.57E-03
A_{S3}	6.98E-03	7.60E-03	8.34E-03	4.31E-03	4.04E-03	5.77E-03	4.92E-03
$S_{33\ +ve}$	1.42E-03	1.56E-03	1.69E-03	1.25E-03	9.19E-04	1.06E-03	9.17E-03
$S_{33\ +ve}$	1.42E-03	1.46E-03	1.44E-03	1.25E-03	9.19E-04	1.06E-03	9.17E-03
S_{22+ve}	2.23E-03	2.25E-03	2.27E-03	2.17E-03	1.68E-03	1.72E-03	1.68E-03
$S_{22\ +ve}$	2.23E-03	2.25E-03	2.27E-03	2.04E-03	1.68E-03	1.72E-03	1.68E-03
z_{33}	1.70E-03	1.79E-03	1.87E-03	1.48E-03	1.08E-03	1.24E-03	1.08E-03
z_{22}	2.58E-03	2.63E-03	2.67E-03	2.39E-03	1.94E-03	2.03E-03	1.94E-03
r_{33}	0.1203	0.1217	0.1229	0.1179	0.1013	0.1044	0.1016
r_{22}	0.1772	0.1747	0.1723	0.1819	0.1768	0.1704	0.1768
xcg	-1.03E-18	-9.93E-19	9.57E-19	-6.72E-03	-2.73E-18	-2.48E-18	-2.73E-18
ycg	-1.76E-18	5.83E-03	0.0114	-1.32E-18	1.91E-19	-6.99E-19	2.87E-19
Xpna	0	5.04E-03	0.0104	0	0	0	0
Ypna	0	0	0	0.0214	0	0	0

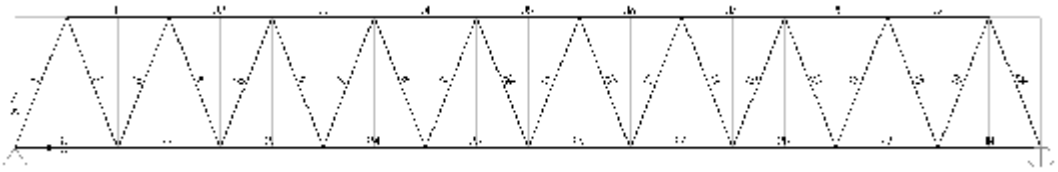

Figure A.A.1: 2D view of bridge with member ID

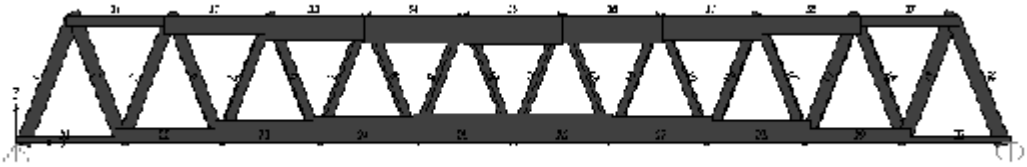

Figure A.A.2: Axial Force Diagram

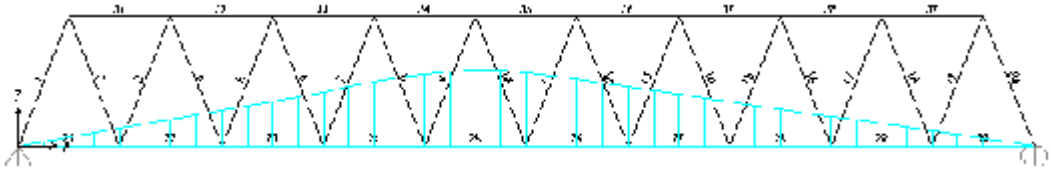

Figure A.A.3: ILD for Axial force of member 25

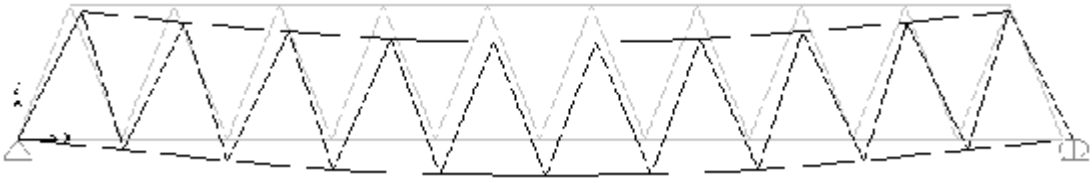

FigureA.A.4: Deformed shape in XZ plane

Table A.A.3: Joint Displacement

Joint	Output Case	Case Type	Step Type	Ux	Uy
Text	Text	Text	Text	m	m
1	ACASE1	LinMoving	Max	0	0
1	ACASE1	LinMoving	Min	0	0
3	ACASE1	LinMoving	Max	0.000403	0
3	ACASE1	LinMoving	Min	0	-0.013632
5	ACASE1	LinMoving	Max	0.001486	0
5	ACASE1	LinMoving	Min	0	-0.026234
7	ACASE1	LinMoving	Max	0.003056	0
7	ACASE1	LinMoving	Min	0	-0.036246
9	ACASE1	LinMoving	Max	0.004928	0
9	ACASE1	LinMoving	Min	0	-0.042549
11	ACASE1	LinMoving	Max	0.006855	0
11	ACASE1	LinMoving	Min	0	-0.044381
13	ACASE1	LinMoving	Max	0.008743	0
13	ACASE1	LinMoving	Min	0	-0.042549
15	ACASE1	LinMoving	Max	0.010487	0
15	ACASE1	LinMoving	Min	0	-0.036246
17	ACASE1	LinMoving	Max	0.011867	0
17	ACASE1	LinMoving	Min	0	-0.026234
19	ACASE1	LinMoving	Max	0.012762	0
19	ACASE1	LinMoving	Min	0	-0.013632
21	ACASE1	LinMoving	Max	0.01308	0
21	ACASE1	LinMoving	Min	0	0

Table A.A.4: Element Forces – Bottom Chords

Member ID	P KN	V2 KN	T KN-M	M3 KN-M	Remarks
21	265.423	240.367	403.004	168.1737	max
	0	-277.243	-402.981	-143.3681	min
22	718.025	233.911	403.0004	152.1267	max.
	0	-239.82	-403	-140.2078	min
23	1058.943	235.064	403.0004	155.9906	max.
	0	-238.201	-403.04	-131.4381	min
24	1281.169	235.586	403.04	157.6402	max.
	0	-237.453	-403.004	-127.739	min
25	1386.522	236.203	403.004	160.3934	max.
	0	-236.496	-403	-123.848	min
26	1386.522	236.497	402.981	160.389	max.
	0	-236.204	-403.04	-123.848	min
27	1281.174	237.456	402.981	157.633	max.
	0	-235.586	-403.004	-127.739	min
28	1058.943	238.208	403.004	155.9802	max.
	0	-235.064	-403.04	-131.442	min
29	717.998	239.828	403.004	152.113	max.
	0	-233.911	-403.004	-140.208	min
30	265.422	227.252	402.981	168.1737	max.
	0	-240.367	-403.004	-143.368	min.

Table A.A.5: Element Forces – Diagonal Member

ID	P max	Pmin	V2max	V2min	M_{max}	M_{min}
1	0.000	-713.779	12.807	-1.433	58.620	-27.401
2	705.131	0.000	8.148	-7.032	30.763	-16.505
3	42.601	-586.844	6.042	-3.599	25.378	-16.899
4	591.952	-38.345	6.839	-3.971	19.229	-27.334
5	75.073	-485.218	6.532	-4.098	28.694	-18.643
6	485.526	-74.013	5.444	-3.900	18.675	-17.328
7	136.024	-383.165	5.426	-3.900	24.098	-17.328
8	385.290	-134.379	5.033	-4.152	19.472	-20.605
9	211.187	-292.594	4.907	-4.203	22.304	-18.086
10	294.057	-209.822	4.506	-4.480	20.635	-18.959
11	294.058	-209.822	4.480	-4.506	18.675	-17.328
12	211.187	-292.594	4.203	-4.907	24.098	-17.328
13	385.286	-134.378	4.152	-5.033	19.472	-20.605
14	136.023	-383.168	3.900	-5.426	24.099	-17.328
15	385.290	-74.013	4.005	-5.444	18.675	-22.172
16	75.073	-485.223	4.098	-6.532	28.696	-18.643
17	591.951	-38.345	3.971	-6.838	19.229	-27.333
18	42.601	-586.838	3.599	-6.042	25.380	-16.899
19	705.130	0.000	7.032	-8.148	30.763	-35.767
20	0.000	-713.770	1.433	-12.807	58.626	-27.402

APPENDIX B

DISPLACEMENT OUT PUT FOR WELDED K- JOINT: ANSYS

Table A.B.1: Coordinate of welded connection

Node No.	Coordinate			Remarks	
	X	Y	Z		
Text	mm	mm	mm		
1455	-24.78	511.21	0.00	Weld1	Bottom chord top and gusset plate connection
6244	-64.15	500.00	10.60		
1551	149.45	504.58	0.00	Weld2	
6248	181.95	500.00	10.60		
1573	395.44	515.38	0.00	Weld3	
6252	428.05	500.00	10.60		
1465	634.61	512.11	0.00	Weld4	
6256	674.15	500.00	10.60		
1399	29.74	82.77	0.00	Weld5	Bottom chord bottom and gusset plate connection
6086	58.90	100.00	10.60		
1382	285.48	75.33	0.00	Weld6	
6090	305.00	100.00	10.60		
1376	528.74	79.55	0.00	Weld7	
6094	551.10	100.00	10.60		
1294	509.89	1073.00	0.00	Weld8	gusset plate and right diagonal member connection parallel to load
12095	528.46	1096.67	9.10		
1374	442.12	945.91	0.00	Weld9	
12091	468.48	944.69	9.10		
1481	374.37	762.35	0.00	Weld10	
11847	408.20	792.70	9.10		
1530	538.24	681.25	0.00	Weld11	Gusset plate and right diagonal
11908	580.85	724.30	9.10		

1461	681.68	784.20	0.00	Weld12	member connection
11930	668.54	777.49	9.10		
1500	3.68	690.70	0.00	Weld13	Left diagonal member and gusset plate connection
17538	16.11	722.45	9.10		
1479	164.77	761.82	0.00	Weld14	
17592	177.84	787.99	9.10		
1280	90.20	1092.46	0.00	Weld15	Gusset plate and left diagonal member connection parallel to load
17608	78.85	1100.71	9.10		
1311	110.53	1028.77	0.00	Weld16	
17606	109.59	1024.96	9.10		
1434	182.64	852.84	0.00	Weld17	
19705	180.16	851.04	5.58		

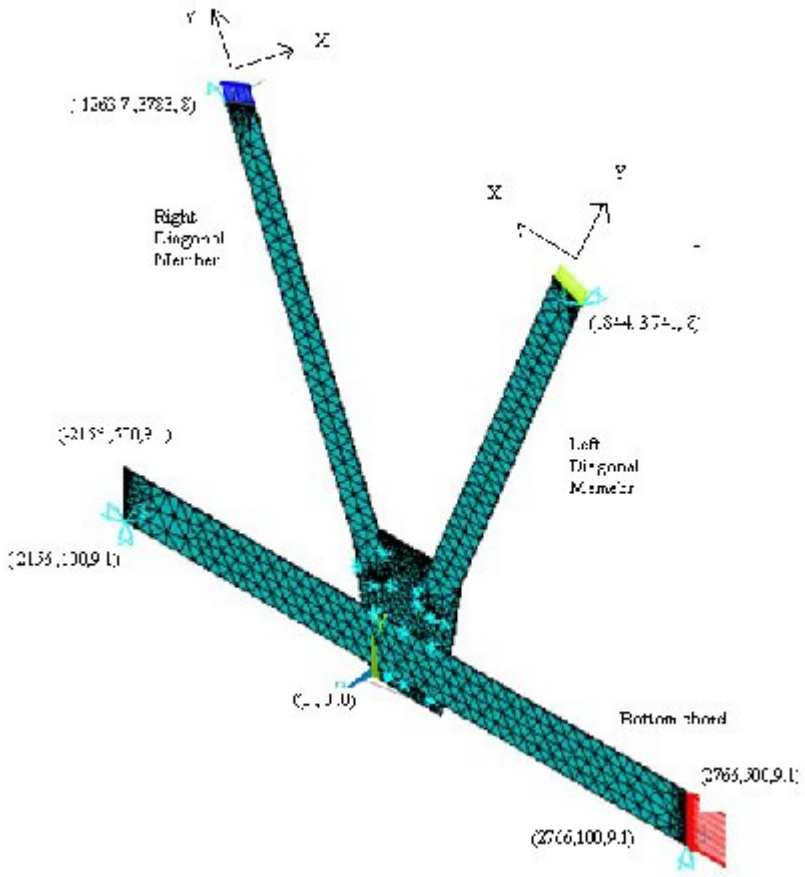

Figure A.B.1: 3D Model of k –Joint, showing the welded point and coordinate system

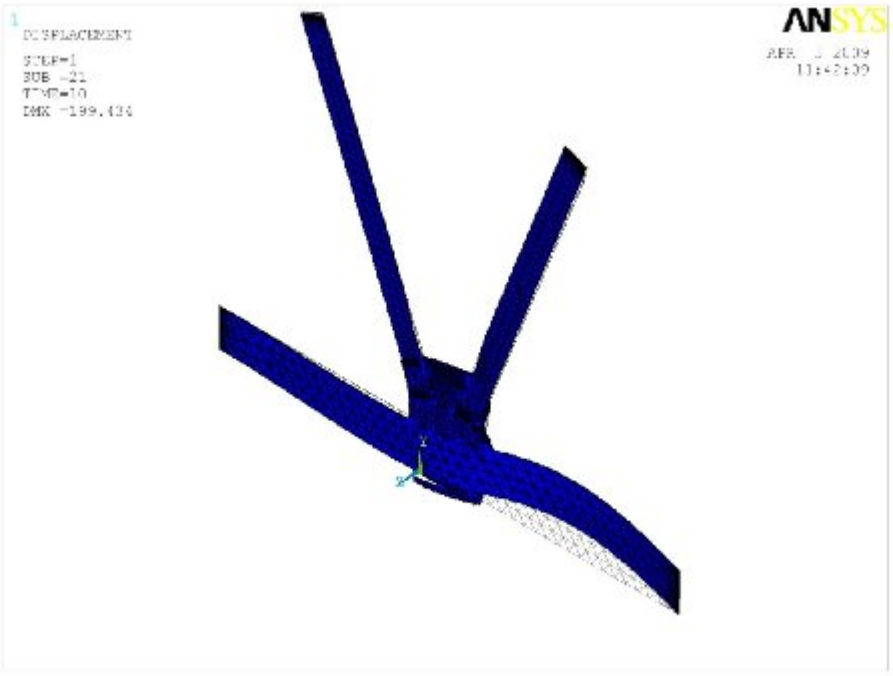

Figure A.B.2: Deformed shape of joint at 5mm weld radius, time=10 sec

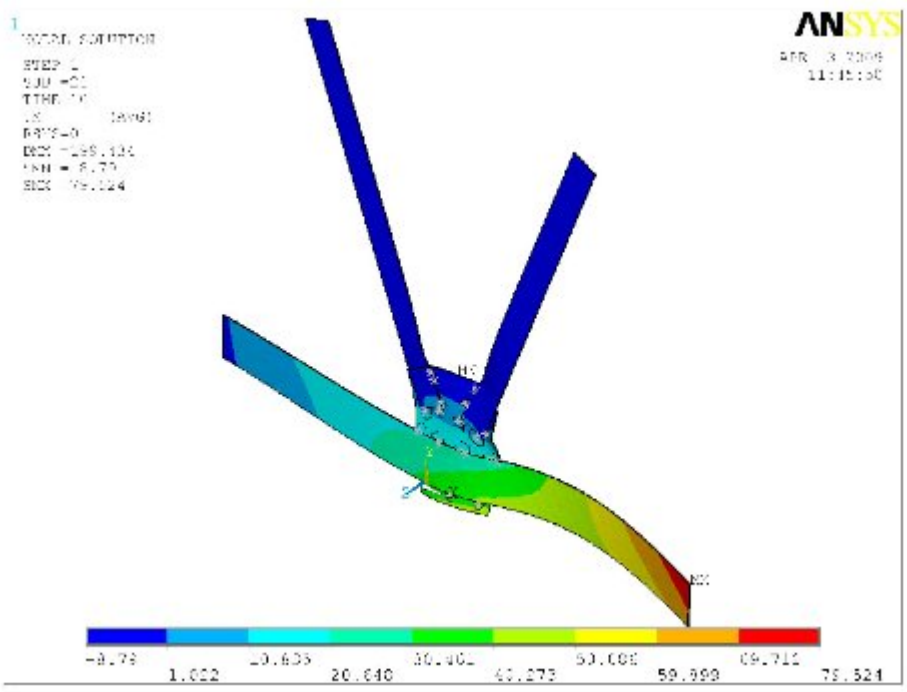

Figure A.B.3: Displacement in x-direction of at 5mm weld radius, time=10 sec

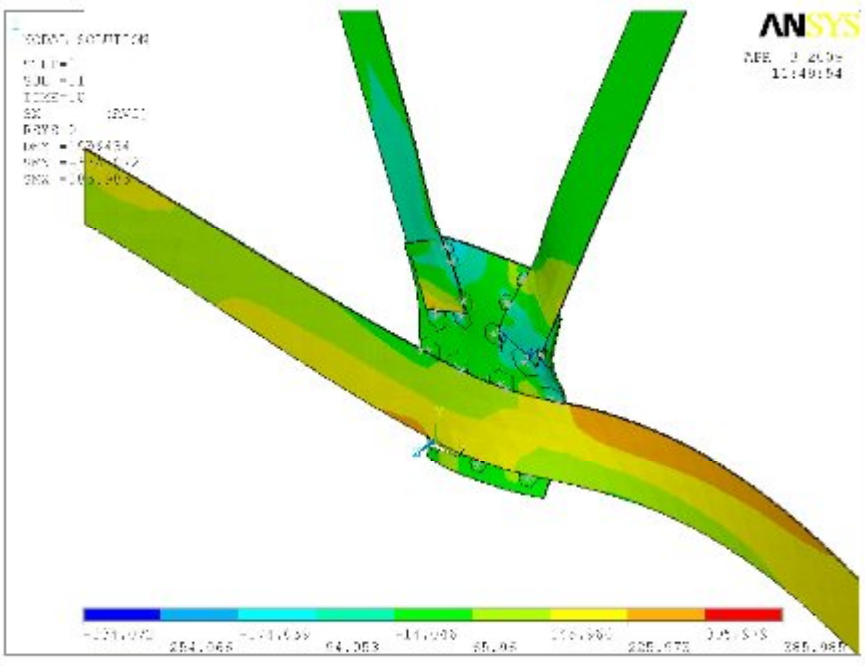

Figure A.B.4: Normal stress in x-direction of at 5mm weld radius, time=10 sec

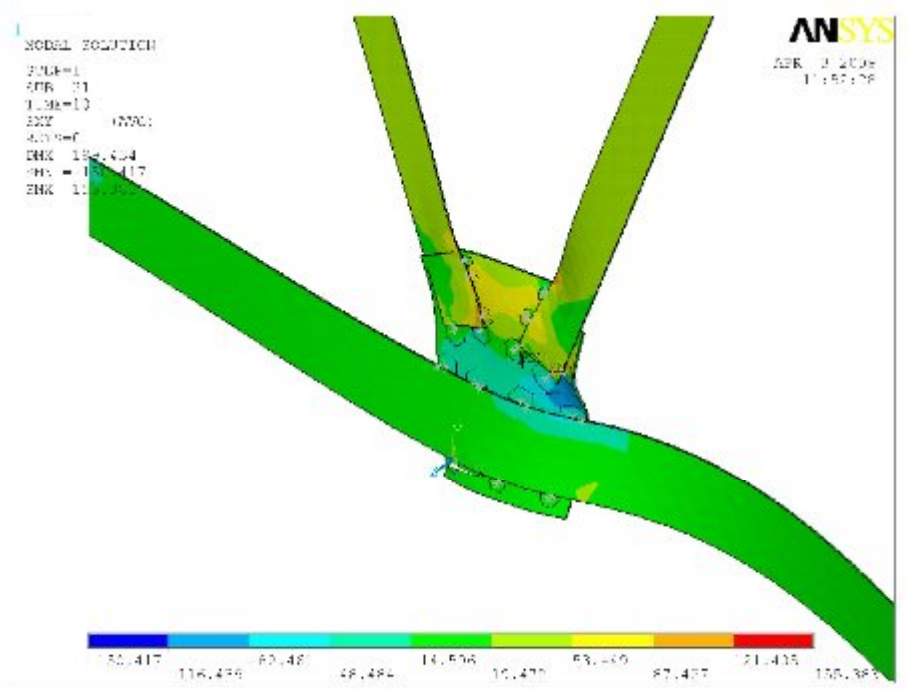

Figure A.B.5: Shear stress in XY plane of at 5mm weld radius, time=10 sec.

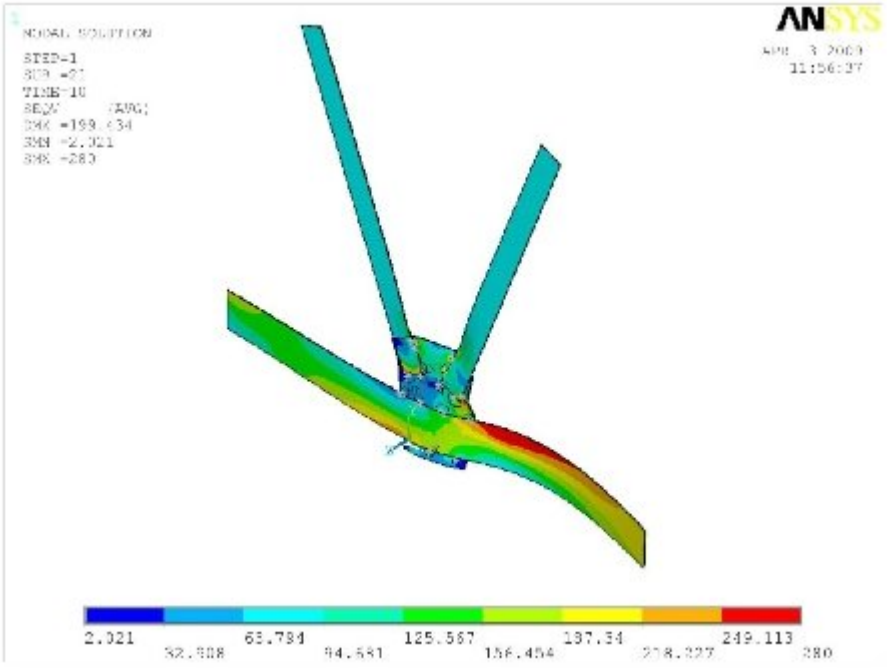

Figure A.B.5: Von-misses stress in of at 5mm weld radius, time=10 sec

Table A.B.2: Displacement in x-direction

S. N0.	Node No.	T=10 second			T= 20 second			Remarks
		weld radius			weld radius			
		2mm	3mm	5mm	2mm	3mm	5mm	
		ux	ux	ux	ux	ux	ux	
1	6210	0.000	0.000	0.000	0.000	0.000	0.000	
2	6212	2.668	2.429	2.247	1.647	1.436	1.308	
3	6214	5.034	4.553	4.184	3.095	2.685	2.423	
4	6216	7.350	6.610	6.044	4.563	3.939	3.530	
5	6218	9.578	8.570	7.803	6.034	5.184	4.620	
6	6220	11.696	10.416	9.446	7.491	6.407	5.682	
7	6222	13.696	12.142	10.969	8.939	7.611	6.720	
8	6224	15.577	13.745	12.369	10.364	8.785	7.724	
9	6226	17.339	15.225	13.645	11.765	9.928	8.693	
10	6228	18.982	16.538	14.800	13.145	11.043	9.631	
11	6230	20.506	17.819	15.832	14.505	12.130	10.536	
12	6232	21.912	18.933	16.742	15.844	13.189	11.409	
13	6234	23.198	19.925	17.529	17.163	14.221	12.250	
14	6236	24.366	20.794	18.193	18.461	15.224	13.058	
15	6238	25.416	21.542	18.733	19.739	16.198	13.829	
16	6240	26.350	22.168	19.146	20.996	17.140	14.553	
17	6242	27.183	22.688	19.428	22.556	18.058	15.185	
18	6244	27.900	23.047	19.556	23.582	19.008	15.820	weld1
19	6246	28.357	23.305	19.759	24.123	19.385	16.152	
20	6248	29.845	24.331	20.657	25.867	20.647	17.209	weld2
21	6250	30.610	24.953	21.256	26.740	21.376	17.879	
22	6252	33.814	27.380	23.307	29.937	23.701	19.705	weld3
23	6254	34.774	28.266	23.978	30.929	24.618	20.387	
24	6256	37.830	30.774	26.889	33.833	26.977	23.157	weld4
25	6258	38.189	31.134	29.085	34.180	27.307	25.219	
26	6260	44.988	39.236	35.578	40.511	34.473	31.013	
27	6262	48.156	42.626	39.162	43.367	37.339	34.049	
28	6264	51.466	46.115	42.658	46.401	40.440	37.182	
29	6266	54.673	49.461	46.001	49.366	43.456	40.227	
30	6268	57.759	52.659	49.195	52.259	46.397	43.190	
31	6270	60.762	55.718	52.249	55.083	49.259	46.076	
32	6272	63.690	58.687	55.215	57.841	52.051	48.891	
33	6274	66.545	61.579	58.103	60.542	54.782	51.645	
34	6276	69.325	64.393	60.914	63.188	57.453	54.335	
35	6278	72.030	67.127	63.645	65.776	60.063	56.962	
36	6280	74.661	69.783	66.298	68.308	62.615	59.527	
37	6282	77.218	72.360	68.873	70.785	65.107	62.031	

38	6284	79.694	74.851	71.363	73.198	67.533	64.465	
39	6286	82.045	77.212	73.723	75.499	69.842	66.782	
40	6288	84.193	79.365	75.875	77.612	71.961	68.907	
41	6130	86.000	81.172	77.682	79.405	73.755	70.705	

APPENDIX C

STRESS OUT PUT FOR FE MODEL OF WELDED K- JOINT: ANSYS

Table A.C.1: Output for bottom chord welded node on top

T= 10 second									
Node number	Weld Radius			Weld Radius			Weld Radius		
	2mm	3mm	5mm	2mm	3mm	5mm	2mm	3mm	5mm
	Sx	Sx	Sx	Sy	Sy	Sy	Sz	Sz	Sz
6244	39.546	22.813	15.084	-20.262	-19.093	-12.445	-4.514	-0.375	-1.932
6248	73.561	54.239	51.095	-17.730	-8.963	7.179	-0.346	1.954	4.732
6252	129.880	98.071	82.883	4.606	2.072	-5.720	8.116	5.533	8.208
6256	120.570	98.206	96.326	13.482	8.527	-15.400	3.452	4.426	3.995

T= 10 second												
Node number	Weld Radius			Weld Radius			Weld Radius			Weld Radius		
	2mm	3mm	5mm	2mm	3mm	5mm	2mm	3mm	5mm	2mm	3mm	5mm
	sxy	sxy	sxy	syz	syz	syz	sxz	sxz	sxz	SEQV	SEQV	SEQV
6244	-0.747	0.074	-0.936	-1.418	-0.512	-0.184	10.577	4.710	3.075	57.379	37.604	52.893
6248	4.200	-1.793	-8.174	-1.766	-2.571	-2.938	17.458	14.710	15.558	90.675	64.770	75.154
6252	5.929	-8.684	-24.116	1.306	-0.314	0.337	21.709	18.655	14.047	200.660	101.550	101.760
6256	-18.665	-43.250	-57.627	1.321	0.290	-2.475	4.499	0.149	2.510	119.300	121.430	119.420

Table A.C.2: Output for gusset plate node connected to top of bottom chord

T= 10 second									
Node number	Weld Radius			Weld Radius			Weld Radius		
	2mm	3mm	5mm	2mm	3mm	5mm	2mm	3mm	5mm
	sx	sx	sx	sy	sy	sy	sz	sz	sz
1455	-19.354	-7.512	14.247	-20.262	-19.093	-12.445	-4.514	-0.375	-1.932
1551	8.629	17.085	36.573	-17.730	-8.963	7.179	-0.346	1.954	4.732
1573	33.436	28.972	25.474	4.606	2.072	-5.720	8.116	5.533	8.208
1465	-39.536	-76.137	-86.485	13.482	8.527	-15.400	3.452	4.426	3.995

T= 10 second												
Node number	Weld Radius			Weld Radius			Weld Radius			Weld Radius		
	2mm	3mm	5mm	2mm	3mm	5mm	2mm	3mm	5mm	2mm	3mm	5mm
	sxy	sxy	sxy	syz	syz	syz	sxz	sxz	sxz	SEQV	SEQV	SEQV
1455	-0.75	0.07	-0.94	-1.42	-0.51	-0.18	10.58	4.71	3.08	42.65	44.37	50.02
1551	4.20	-1.79	-8.17	-1.77	-2.57	-2.94	17.46	14.71	15.56	39.47	41.51	79.22
1573	5.93	-8.68	-24.12	1.31	-0.31	0.34	21.71	18.66	14.05	40.19	58.42	97.75
1465	-18.67	-43.25	-57.63	1.32	0.29	-2.47	4.50	0.15	2.51	39.92	83.57	121.6

Table A.C.3: Output for bottom chord welded node on bottom

T= 10 second									
Node number	Weld Radius			Weld Radius			Weld Radius		
	2mm	3mm	5mm	2mm	3mm	5mm	2mm	3mm	5mm
	sx	sx	sx	sy	sy	sy	sz	sz	sz
6086	153.09	149.76	125.30	12.66	13.67	0.41	6.84	6.88	5.83
6090	136.47	132.11	107.69	7.75	3.01	3.01	7.23	7.43	5.79
6094	115.47	102.09	92.45	-9.54	-6.45	-1.40	-9.85	-12.97	-17.88

T= 10 second												
Node number	Weld Radius			Weld Radius			Weld Radius			Weld Radius		
	2mm	3mm	5mm	2mm	3mm	5mm	2mm	3mm	5mm	2mm	3mm	5mm
	sxy	sxy	sxy	syz	syz	syz	sxz	sxz	sxz	SEQV	SEQV	SEQV
6086	-43.5	-42.8	-31.9	-3.1	-3.8	-3.37	13.8	13.69	9.93	141.30	162.41	211.28
6090	-19.8	-19.5	-15.3	-1.5	-1.8	-1.24	5.22	3.427	1.73	114.19	132.25	160.79
6094	-8.49	0.27	5.063	2.52	1.04	0.186	13.6	14.95	18.3	112.97	117.21	100.11

Table A.C.4: Output for gusset plate node connected to bottom of bottom chord

T= 10 second									
Node number	Weld Radius			Weld Radius			Weld Radius		
	2mm	3mm	5mm	2mm	3mm	5mm	2mm	3mm	5mm
	sx	sx	sx	sy	sy	sy	sz	sz	sz
1399	-12.91	-12.90	-4.83	-15.52	-15.33	-7.41	2.80	0.74	5.83
1382	27.45	28.22	6.02	8.12	0.44	-8.06	-3.20	-2.20	5.79
1376	3.92	17.77	24.11	-4.62	2.34	8.13	-0.31	0.04	-17.88

T= 10 second												
Node number	Weld Radius			Weld Radius			Weld Radius			Weld Radius		
	2mm	3mm	5mm	2mm	3mm	5mm	2mm	3mm	5mm	2mm	3mm	5mm
	sxy	sxy	sxy	syz	syz	syz	sxz	sxz	sxz	SEQV	SEQV	SEQV
1399	2.24	0.30	-1.65	0.62	-0.62	-0.70	-8.68	-10.28	-5.14	9.34	24.68	31.27
1382	-2.61	-1.50	-5.51	2.58	1.47	1.25	-0.70	-1.13	-0.89	13.93	30.05	32.15
1376	-2.74	7.30	12.41	0.19	-0.09	-0.03	-2.03	1.66	4.46	18.45	21.21	46.25

Table A.C.5: Output for Right Diagonal member welded node on top

T= 10 second									
Node number	Weld Radius			Weld Radius			Weld Radius		
	2mm	3mm	5mm	2mm	3mm	5mm	2mm	3mm	5mm
	sx	sx	sx	sy	sy	sy	sz	sz	sz
12095	-30.12	-21.86	6.73	49.12	-39.38	34.55	-63.04	87.53	25.60
12091	16.67	-7.25	15.25	-82.47	-156.19	-27.12	-117.82	-72.99	-26.63
11847	49.39	59.24	-95.74	93.29	-25.88	-49.82	50.67	-14.39	-81.83

T= 10 second												
Node number	Weld Radius			Weld Radius			Weld Radius			Weld Radius		
	2mm	3mm	5mm	2mm	3mm	5mm	2mm	3mm	5mm	2mm	3mm	5mm
	sxy	sxy	sxy	syz	syz	syz	sxz	sxz	sxz	SEQV	SEQV	SEQV
12095	-10.12	-12.1	7.3039	28.868	33.333	33.53	15.009	12.893	0.5077	119	139.05	66.259
12091	29.23	-42.5	6.2178	-38.667	-18.773	-0.38	42.888	-24.58	-3.675	172.2	164.25	45.819
11847	25.22	80.398	-63.52	-16.423	-62.518	-17.3	-104.2	-40.22	122	235.05	229.48	251.59

Table A.C.6: Output for Left Diagonal member welded node on top

T= 10 second									
Node number	Weld Radius			Weld Radius			Weld Radius		
	2mm	3mm	5mm	2mm	3mm	5mm	2mm	3mm	5mm
	sx	sx	sx	sy	sy	sy	sz	sz	sz
17608	9.15	10.17	22.21	-68.61	-53.51	-58.45	-48.46	-70.32	-47.94
17606	-7.66	-7.73	-9.78	16.36	-79.47	-100.18	-67.59	7.47	-5.20
19705	16.31	-7.31	-0.76	182.93	21.56	-59.64	52.93	218.75	179.50

T= 10 second												
Node number	Weld Radius			Weld Radius			Weld Radius			Weld Radius		
	2mm	3mm	5mm	2mm	3mm	5mm	2mm	3mm	5mm	2mm	3mm	5mm
	sxy	sxy	sxy	syz	syz	syz	sxz	sxz	sxz	SEQV	SEQV	SEQV
17608	9.09	3.56	15.91	-26.30	-35.47	-52.50	-5.12	-9.86	4.46	87.00	99.24	123.68
17606	-4.44	-5.29	-0.12	-18.84	-31.20	-50.08	5.93	6.51	2.91	84.28	99.90	128.32
19705	115.71	-3.41	1.07	5.62	-29.21	-47.84	-18.32	-89.65	-61.92	253.52	268.54	254.84

Table A.C.7: Output for bottom chord welded node on top

T= 20 second									
Node number	Weld Radius			Weld Radius			Weld Radius		
	2mm	3mm	5mm	2mm	3mm	5mm	2mm	3mm	5mm
	sx	sx	sx	sy	sy	sy	sz	sz	sz
6244	63.07	48.11	38.75	-12.19	-3.50	8.94	-0.61	0.75	-2.94
6248	78.92	58.24	52.18	-10.41	-1.25	12.98	-1.86	0.33	2.94
6252	124.90	87.04	67.91	6.22	-3.25	-10.63	5.87	3.69	5.74
6256	112.22	85.75	80.00	9.27	-7.34	-21.60	3.13	3.99	3.59

T= 20 second												
Node number	Weld Radius			Weld Radius			Weld Radius			Weld Radius		
	2mm	3mm	5mm	2mm	3mm	5mm	2mm	3mm	5mm	2mm	3mm	5mm
	sxy	sxy	sxy	syz	syz	syz	sxz	sxz	sxz	SEQV	SEQV	SEQV
6244	3.376	2.369	-1.173	-1.135	-1.218	-1.233	13.887	9.7358	8.781	74.799	52.893	40.801
6248	-9.109	-16.76	-20.64	-4.395	-4.8607	-3.57	22.313	19.611	19.08	96.412	75.154	67.627
6252	-27.51	-22.42	-38.63	-0.067	-1.2469	0.7877	2.7748	18.736	13.52	126.38	101.76	102.04
6256	-23.32	-44.52	-59.81	0.4218	-1.6003	-1.595	4.2451	-0.5515	2.161	115.59	119.42	100.36

Table A.C.8: Output for gusset plate node connected to top of bottom chord

T= 20 second									
Node number	Weld Radius			Weld Radius			Weld Radius		
	2mm	3mm	5mm	2mm	3mm	5mm	2mm	3mm	5mm
	sx	sx	sx	sy	sy	sy	sz	sz	sz
1455	5.89	14.25	15.14	12.37	31.02	49.06	-1.05	-2.43	-4.74
1551	28.64	36.57	43.65	9.53	23.22	37.23	-4.38	-4.34	-3.49
1573	33.82	25.47	26.93	7.00	7.89	10.49	9.71	12.40	12.19
1465	-48.28	-86.49	-100.30	-61.31	-106.49	-113.05	-4.26	-6.79	-9.47

T= 20 second												
Node number	Weld Radius			Weld Radius			Weld Radius			Weld Radius		
	2mm	3mm	5mm	2mm	3mm	5mm	2mm	3mm	5mm	2mm	3mm	5mm
	sxy	sxy	sxy	syz	syz	syz	sxz	sxz	sxz	SEQV	SEQV	SEQV
6244	-26.39	-23.49	-22.53	0.7642	1.6768	4.0186	-0.052	-0.0975	0.379	47.176	50.024	61.577
6248	-36.62	-40.54	-41.28	3.3575	2.3748	0.4751	0.6968	2.8048	5.072	69.886	79.22	84.563
6252	-40.37	-55.64	-56.92	-3.921	-2.5168	0.8152	-0.351	0.397	0.862	74.758	97.753	99.842
6256	-13.32	-42.55	-46.66	-8.035	-9.4236	-6.374	13.353	15.875	21.14	62.555	121.66	132.53

Table A.C.9: Output for bottom chord welded node on bottom chord

T= 20 second									
Node number	Weld Radius			Weld Radius			Weld Radius		
	2mm	3mm	5mm	2mm	3mm	5mm	2mm	3mm	5mm
	sx	sx	sx	sy	sy	sy	sz	sz	sz
6086	131.7	125.3	137.92	1.0966	0.4124	-7.802	6.0496	5.8334	-1.4375
6090	116.6	107.69	128.13	7.1571	3.0113	-9.248	5.429	5.7933	-3.1461
6094	97.569	92.454	80.152	-0.449	-1.4015	-7.207	-15.831	-17.883	-16.348

T= 20 second												
Node number	Weld Radius			Weld Radius			Weld Radius			Weld Radius		
	2mm	3mm	5mm	2mm	3mm	5mm	2mm	3mm	5mm	2mm	3mm	5mm
	sxy	sxy	sxy	syz	syz	syz	sxz	sxz	sxz	SEQV	SEQV	SEQV
6086	-31.45	-42.81	-18.83	-3.25	-3.37	-1.25	10.45	9.93	1.80	141.30	136.06	147.06
6090	-15.09	-19.45	-3.12	-0.98	-1.24	-5.04	2.86	1.73	-14.12	114.19	107.06	137.72
6094	-0.41	0.27	10.84	1.34	0.19	-0.11	16.59	18.30	16.72	112.97	111.44	102.23

Table A.C.10: Output for gusset plate node connected to bottom of bottom chord

T= 20 second									
Node number	Weld Radius			Weld Radius			Weld Radius		
	2mm	3mm	5mm	2mm	3mm	5mm	2mm	3mm	5mm
	sx	sx	sx	sy	sy	sy	sz	sz	sz
1399	-4.78	-4.83	-4.45	-7.17	-7.41	-4.34	0.64	0.74	1.99
1382	5.61	6.02	7.19	-2.74	-8.06	-15.94	-1.19	-2.20	-3.01
1376	16.78	24.11	31.01	4.76	8.13	8.48	-0.09	0.04	-0.35

T= 20 second												
Node number	Weld Radius			Weld Radius			Weld Radius			Weld Radius		
	2mm	3mm	5mm	2mm	3mm	5mm	2mm	3mm	5mm	2mm	3mm	5mm
	sxy	sxy	sxy	syz	syz	syz	sxz	sxz	sxz	SEQV	SEQV	SEQV
1399	0.19242	-1.65	-6.162	-0.4643	-0.7	-0.121	-3.6365	-5.137	-8.8201	9.34	11.87	19.70
1382	-6.2799	-5.51	-4.651	2.1759	1.25	-0.205	-0.8994	-0.892	-2.599	13.93	15.75	22.11
1376	6	12.409	19.864	0.214	-0.03	-0.811	1.7965	4.4588	7.1076	18.45	31.17	46.05

Table A.C.11: Output for Right Diagonal member welded node on top

T= 20 second									
Node number	Weld Radius			Weld Radius			Weld Radius		
	2mm	3mm	5mm	2mm	3mm	5mm	2mm	3mm	5mm
	sx	sx	sx	sy	sy	sy	sz	sz	sz
12095	25.818	6.7282	1.7423	68.46	34.55	27.994	-20.94	25.6	42.56
12091	2.0236	15.253	2.3	-14.13	-27.124	-34.45	-47.3	-26.63	-31.11
11847	-102.1	-95.737	-117.01	-49.5	-49.817	-109.5	-109.5	-81.83	-103.2

T= 20 second												
Node number	Weld Radius			Weld Radius			Weld Radius			Weld Radius		
	2mm	3mm	5mm	2mm	3mm	5mm	2mm	3mm	5mm	2mm	3mm	5mm
	sxy	sxy	sxy	syz	syz	syz	sxz	sxz	sxz	SEQV	SEQV	SEQV
12095	14.50	7.30	4.92	-3.37	33.53	42.27	15.01	12.89	0.51	86.57	66.26	84.51
12091	25.30	6.22	-3.96	2.16	-0.38	-1.62	42.89	-24.58	-3.68	66.23	45.82	42.30
11847	-75.49	-63.52	47.92	-29.79	-17.29	-67.60	-104.21	-40.22	122.00	248.84	251.59	272.54

Table A.C.12: Output for Left Diagonal member welded node on top

T= 20 second									
Node number	Weld Radius			Weld Radius			Weld Radius		
	2mm	3mm	5mm	2mm	3mm	5mm	2mm	3mm	5mm

	sx	sx	sx	sy	sy	sy	sz	sz	sz
17608	-4.729	-3.7783	-14.45	-2.5489	-21.162	-32.84	-58.218	-77.56	-93.4
17606	19.633	11.931	10.441	64.199	44.466	23.1	-46.788	-47.41	-42.71
19705	8.2552	-6.7694	2.213	93.862	126.89	72.5	147.74	162.21	114.41

T= 20 second												
Node number	Weld Radius			Weld Radius			Weld Radius			Weld Radius		
	2mm	3mm	5mm	2mm	3mm	5mm	2mm	3mm	5mm	2mm	3mm	5mm
	sxy	sxy	sxy	syz	syz	syz	sxz	sxz	sxz	SEQV	SEQV	SEQV
17608	0.577	-0.128	-9.777	10.897	13.45	22.052	-4.223	-8.446	-1.6942	61.711	75.36	85.46
17606	-0.091	0.1717	1.2836	30.282	22.32	13.742	-6.6379	-5.017	-3.1907	11.49	90.57	66.01
19705	-83.362	-22.15	-13.4	69.522	81.59	81.826	-81.055	-51.94	-55.085	264.39	231.5	198.4

APPENDIX D

FATIGUE DAMAGE CALCULATION OF WELDED NODE

Table A.D.1: Fatigue Calculation of 2mm weld radius K-joint

S.N	Node number	Alt. stress	No. of cycles reuired	No. of cycles applied	Damage (ni/Ni)	No. of cycles applied	Damage (ni/Ni)	No. of cycles applied	Damage (ni/Ni)	No. of cycles applied	Damage (ni/Ni)
				1.00E+05		6.00E+05		2.00E+06		1.00E+07	
1	1455	27.223	2.38E+07		0.0042		0.0252		0.0840		0.4201
2	6244	10.318	1.00E+08		0.0010		0.0060		0.0200		0.1000
3	1551	25.683	3.12E+07		0.0032		0.0192		0.0641		0.3203
4	6248	15.038	1.00E+08		0.0010		0.0600		0.0200		0.1000
5	1573	24.631	3.79E+07		0.0026		0.0158		0.0527		0.2636
6	6252	12.427	1.00E+08		0.0010		0.0060		0.0200		0.1000
7	1465	18.873	1.00E+08		0.0010		0.0060		0.0200		0.1000
8	6256	6.903	1.00E+08		0.0010		0.0060		0.0200		0.1000
9	1399	6.536	1.00E+08		0.0010		0.0060		0.0200		0.1000
10	6086	23.802	4.48E+07		0.0023		0.0135		0.0450		0.2248
11	1382	10.945	1.00E+08		0.0010		0.0060		0.0200		0.1000
12	6090	14.181	1.00E+08		0.0010		0.0060		0.0200		0.1000
13	1376	10.897	1.00E+08		0.0010		0.0060		0.0200		0.1000
14	6094	18.197	1.00E+08		0.0010		0.0060		0.0200		0.1000
15	1294	128.69	1.00E+05		1.0000		6.0000		20.0000		100.000
16	12095	112.03	1.00E+05		1.0000		6.0000		20.0000		100.000
17	1374	87.993	1.00E+05		0.9997		5.9771		19.9930		99.9652
18	12091	109.41	1.00E+05		1.0000		6.0000		20.0000		100.000
19	1481	41.392	3.38E+06		0.0239		0.1778		0.5927		2.9633
20	11847	133.95	1.00E+05		1.0000		6.0000		20.0000		100.000
21	1530	22.575	5.69E+07		0.0018		0.0105		0.0351		0.1756
22	11908	26.403	2.74E+07		0.0036		0.0218		0.0723		0.3645
23	1461	21.826	6.66E+07		0.0015		0.0090		0.0300		0.1509
24	11930	93.524	1.00E+05		1.0000		6.0000		20.0000		100.000
25	1500	14.161	1.00E+08		0.0010		0.0060		0.0200		0.1000

26	17538	122.44	1.00E+05		1.0000		6.0000		20.0000		100.000
27	1479	30.221	1.46E+07		0.0068		0.0410		0.1366		0.6830
28	17592	32.979	9.75E+06		0.0103		0.0615		0.2051		1.0257
29	1280	74.108	2.24E+05		0.4497		2.6980		8.9934		44.9669
30	17608	50.057	1.39E+06		0.0718		0.4310		1.4368		7.1838
31	1311	72.416	2.49E+05		0.0402		2.4104		8.3305		40.1673
32	17606	120.61	1.00E+05		1.0000		6.0000		20.0000		100.000
33	1434	40.415	3.77E+06		0.0265		0.1590		0.5301		2.6503
34	19705	126.16	1.00E+05		1.0000		6.0000		20.0000		100.000

Table A.D.2: Fatigue Calculation of 3mm weld radius K-joint

S.N	Node number	Alt. stress	No. of cycles reuired	No. of cycles applied	Damage (ni/Ni)	No. of cycles applied	Damage (ni/Ni)	No. of cycles applied	Damage (ni/Ni)	No. of cycles applied	Damage (ni/Ni)
				1.00E+05		6.00E+05		2.00E+06		1.00E+07	
1	1455	31.022	1.30E+07		0.00771		0.04629		0.1542		0.7710

2	6244	12.773	1.00E+08		0.001		0.006		0.02		0.1000
3	1551	24.741	3.72E+07		0.00269		0.01615		0.0538		0.2690
4	6248	16.778	1.00E+08		0.001		0.006		0.02		0.1000
5	1573	25.538	3.21E+07		0.00312		0.01872		0.0624		0.3120
6	6252	13.487	1.00E+08		0.001		0.006		0.02		0.1000
7	1465	22.002	6.41E+07		0.00156		0.00935		0.0312		0.1560
8	6256	10.955	1.00E+08		0.001		0.006		0.02		0.1000
9	1399	6.4095	1.00E+08		0.001		0.006		0.02		0.1000
10	6086	24.176	4.14E+07		0.00242		0.0145		0.0484		0.2420
11	1382	11.806	1.00E+08		0.001		0.006		0.02		0.1000
12	6090	14.643	1.00E+08		0.001		0.006		0.02		0.1000
13	1376	6.8175	1.00E+08		0.001		0.006		0.02		0.1000
14	6094	10.833	1.00E+08		0.001		0.006		0.02		0.1000
15	1294	93.404	1.00E+05		1		6		20		100.0000
16	12095	77.298	1.84E+05		0.5449		3.2694		10.898		54.4900
17	1374	89.6	1.00E+05		1		6		20		100.0000
18	12091	80.488	1.52E+05		0.65719		3.94314		13.1438		65.7190
19	1481	37.398	5.42E+06		0.01845		0.1107		0.369		1.8450
20	11847	133.42	1.00E+05		1		6		20		100.0000
21	1530	26.905	2.52E+07		0.00398		0.02386		0.0796		0.3980
22	11908	27.782	2.17E+07		0.00462		0.0277		0.0924		0.4620
23	1461	14.23	1.00E+08		0.001		0.006		0.02		0.1000
24	11930	90.149	1.00E+05		1		6		20		100.0000
25	1500	13.679	1.00E+08		0.001		0.006		0.02		0.1000
26	17538	143.84	1.00E+05		1		6		20		100.0000
27	1479	31.757	1.16E+07		0.0086		0.05162		0.172		0.8600
28	17592	24.416	3.95E+07		2.50E-03		0.01519		0.05		0.2500
29	1280	83.829	1.26E+05		0.79678		4.7807		15.9356		79.6780
30	17608	52.596	1.11E+06		0.0904		0.54238		1.808		9.0400

31	1311	74.575	2.17E+05		0.46098		2.7659		9.2196		46.0980
32	17606	110.76	1.00E+05		1		6		20		100.0000
33	1434	40.354	3.80E+06		0.02632		0.15792		0.5264		2.6320
34	19705	136.26	1.00E+05		1		6		20		100.0000

Table A.D.3: Fatigue Calculation of 5mm weld radius K-joint

S.N	Node number	Alt. stress	No. of cycles reuired	No. of cycles applied	Damage (ni/Ni)	No. of cycles applied	Damage (ni/Ni)	No. of cycles applied	Damage (ni/Ni)	No. of cycles applied	Damage (ni/Ni)
				1.00E+05		6.00E+05		2.00E+06		1.00E+07	
1	1455	31.778	1.16E+07		0.00863		0.05178		0.1726		0.8630

2	6244	14.417	1.00E+08		0.001		0.006		0.02		0.1000
3	1551	20.66	8.60E+07		0.00116		0.00696		0.0232		0.1160
4	6248	14.197	1.00E+08		0.001		0.006		0.02		0.1000
5	1573	21.341	7.39E+07		0.00135		0.0081		0.027		0.1350
6	6252	14.984	1.00E+08		0.001		0.006		0.02		0.1000
7	1465	19.504	1.00E+08		0.001		0.006		0.02		0.1000
8	6256	6.0919	1.00E+08		0.001		0.006		0.02		0.1000
9	1399	5.9116	1.00E+08		0.001		0.006		0.02		0.1000
10	6086	32.216	1.09E+07		0.0092		0.0552		0.184		0.9200
11	1382	8.2182	1.00E+08		0.001		0.006		0.02		0.1000
12	6090	12.14	1.00E+08		0.001		0.006		0.02		0.1000
13	1376	2.32	1.00E+08		0.001		0.006		0.02		0.1000
14	6094	4.3916	1.00E+08		0.001		0.006		0.02		0.1000
15	1294	73.933	2.26E+05		0.4427		2.6562		8.854		44.2700
16	12095	68.757	3.17E+05		0.31525		1.8915		6.305		31.5250
17	1374	86.802	1.07E+05		0.93878		5.63268		18.7756		93.8780
18	12091	75.925	2.00E+05		0.50135		3.0081		10.027		50.1350
19	1481	35.453	6.95E+06		0.01438		0.08628		0.2876		1.4380
20	11847	76.173	1.96E+05		0.50904		3.05424		10.1808		50.9040
21	1530	19.541	1.00E+08		0.001		0.006		0.02		0.1000
22	11908	19.913	1.00E+08		0.001		0.006		0.02		0.1000
23	1461	17.948	1.00E+08		0.001		0.006		0.02		0.1000
24	11930	76.218	1.96E+05		0.51044		3.06264		10.2088		51.0440
25	1500	11.611	1.00E+08		0.001		0.006		0.02		0.1000
26	17538	100.8	1.00E+05		1.00		6		20		100.0000
27	1479	30.431	1.42E+07		0.00706		0.04236		0.1412		0.7060
28	17592	77.723	1.79E+05		0.55935		3.3561		11.187		55.9350
29	1280	82.862	1.33E+05		0.75469		4.52814		15.0938		75.4690
30	17608	83.594	1.27E+05		0.78637		4.71822		15.7274		78.6370

31	1311	77.234	1.84E+05		0.54307		3.25842		10.8614		54.3070
32	17606	105.49	1.00E+05		1		6		20		100.0000
33	1434	36.163	6.34E+06		0.01577		0.09462		0.3154		1.5770
34	19705	128.92	1.00E+05		1		6		20		100.0000

Table A.D.4: Fatigue damage of different weld radius in same alt. stress in bottom chord

Bottom Chord welded node - Node 1455				
Weld radius		2mm	3mm	5mm
Alt. stress (Mpa)		27.223	27.2230	27.223
number of cycles	1.00E+05	0.0042	0.0037	0.0036
	6.00E+05	0.0252	0.0222	0.0216
	2.00E+06	0.0840	0.0739	0.0721
	1.00E+07	0.4201	0.3696	0.3603

Table A.D.5: Fatigue damage of different weld radius in same alt. stress in gusset plate

Gusset plate Node 6244 welded with node 1455				
Weld radius		2mm	3mm	5mm
Alt. stress (Mpa)		10.318	10.3180	10.318
number of cycles	1.00E+05	0.0010	0.0008	0.0007
	6.00E+05	0.0060	0.0048	0.0043
	2.00E+06	0.0200	0.0162	0.0143
	1.00E+07	0.1000	0.0808	0.0716

Table A.D.6: Fatigue damage of different weld radius in same alt. stress in Diagonal Members

Diagonal member welded node 1481				
Weld radius		2mm	3mm	5mm
Alt. stress (Mpa)		41.392	41.392	41.392
number of cycles	1.00E+05	0.0239	0.0135	0.0105
	6.00E+05	0.1778	0.1002	0.0781
	2.00E+06	0.5927	0.3339	0.2604
	1.00E+07	2.9633	1.6696	1.3018

APPENDIX E

DESCRIPTION ABOUT THE ELEMENT USED FOR MODELING

SOLID95 Element Description

SOLID95 is a higher order version of the 3-D 8-node solid element SOLID45. It can tolerate irregular shapes without as much loss of accuracy. SOLID95 elements have compatible displacement shapes and are well suited to model curved boundaries.

The element is defined by 20 nodes having three degrees of freedom per node: translations in the nodal x, y, and z directions. The element may have any spatial orientation. SOLID95 has plasticity, creep, stress stiffening, large deflection, and large strain capabilities. Various printout options are also available.

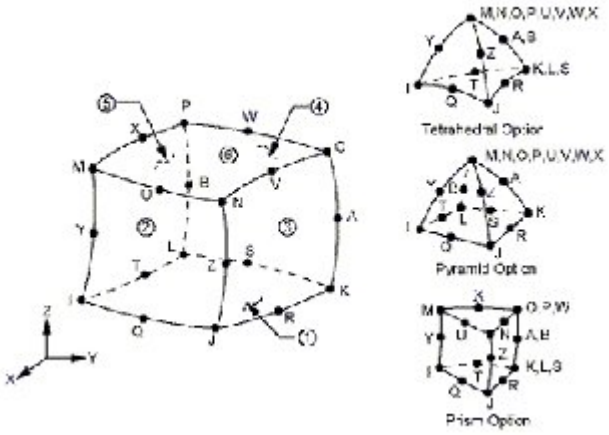

Figure A.E.1: SOLID95

BEAM188 Element Description

BEAM188 is suitable for analyzing slender to moderately stubby/thick beam structures. This element is based on Timoshenko beam theory. Shear deformation effects are included.

BEAM188 is a linear (2-node) or a quadratic beam element in 3-D. BEAM188 has six or seven degrees of freedom at each node, with the number of degrees of freedom depending on the value of KEYOPT(1). When KEYOPT (1) = 0 (the default), six degrees of freedom occur at each node. These include translations in the x, y, and z directions and rotations about the x, y, and z directions. When KEYOPT (1) = 1, a seventh degree of freedom (warping magnitude) is also considered. This element is well-suited for linear, large rotation, and/or large strain nonlinear applications.

BEAM188 includes stress stiffness terms, by default, in any analysis with NLGEOM, ON. The provided stress stiffness terms enable the elements to analyze flexural, lateral, and torsional stability problems (using eigenvalue buckling or collapse studies with arc length methods).BEAM188 can be used with any beam cross-section defined via SECTYPE, SECDATA, SECOFFSET, SECWRITE, and SECREAD. The cross-section associated with the beam may be linearly tapered.
Elasticity, creep, and plasticity models are supported (irrespective of cross-section subtype). A cross-section associated with this element type can be a built-up section referencing more than one material. BEAM188 ignores any real constant data beginning with Release 6.0. See the SECCONTROLS command for defining the transverse shear stiffness, and added mass.

TARGE170 Element Description

TARGE170 is used to represent various 3-D “target” surfaces for the associated contact elements (CONTA173, CONTA174, CONTA175, and CONTA176). The contact elements themselves overlay the solid elements describing the boundary of a deformable body and are potentially in contact with the target surface, defined by TARGE170. This target surface is discredited by a set of target segment elements (TARGE170) and is paired with its associated contact surface via a shared real constant set. You can impose any translational or rotational displacement, temperature, voltage, and magnetic potential on the target segment element. You can also impose forces and moments on target elements. See TARGE170 in the ANSYS, Inc. Theory Reference for more details about this element. To represent 2-D target surfaces, use TARGE169, a 2-D target segment element.

For rigid target surfaces, these elements can easily model complex target shapes. For flexible targets, these elements will overlay the solid elements describing the boundary of the deformable target body.

CONTA175 Element Description

CONTA175 may be used to represent contact and sliding between two surfaces (or between a node and a surface, or between a line and a surface) in 2-D or 3-D. The element is applicable to 2-D or 3-D structural and coupled field contact analyses. This element is located on the surfaces of solid, beam, and shell elements. 3-D solid elements with midside nodes are not supported. Contact occurs when the element surface penetrates one of the target segment elements (TARGE169, TARGE170) on a specified target surface. Coulomb and shear stress friction is allowed. See CONTA175 in the ANSYS, Inc. Theory Reference for more details about this element.

CODE FOR WELD SIMULATION: ANSYS APDL

```
MP, EX, 3,200000              !  Weld material properties
MP, NUXY, 3, 0.3
SECTYPE, 3, beam, csolid      ! Define a circular solid beam section
SECDATA, 2                    ! Beam circular radius
ET, 3,188                     ! Element type for a deformable weld
TYPE, 3
MAT, 3
SECNUM, 3
*SET, NODE1, 9000             ! Define parameter for node number
N, NODE1, X, Y, Z             ! Define weld node
SWGEN, ECOMP, SWRD, NCM1, NCM2, SND1, SND2, SHRD
                                        !  Weld name = ECOMP
                                       ! Radius (SWRD) = 2
                                       !  Welded surfaces = NCM1 and NCM2
                                      ! Welded node = SND1 and SND2
```

APPENDIX F

S-N CURVE USED FOR FATIGUE DAMAGE CALCULATION

Table 6 Values of f and N for Fluctuating Stresses — Class F Constructional Details
(Clauses 5.2.2, 5.3.1, 5.3.2 and 5.4)

f_{Min}/f_{Max} \ N (1)	f or f_{Max} Tensile, MPa					f or f_{Max} Compressive, MPa				
	10^4 cycles (2)	6×10^4 cycles (3)	2×10^5 cycles (4)	10^5 cycles (5)	10^6 cycles (6)	10^4 cycles (7)	6×10^4 cycles (8)	2×10^5 cycles (9)	10^5 cycles (10)	10^6 cycles (11)
1.0	432.4	432.4	432.4	432.4	432.4	–	–	–	–	–
0.9	377.1	330.3	296.4	260.0	190.9	–	–	–		
0.8	334.3	267.3	225.5	175.8	122.5	–	–	–	–	–
0.7	300.2	224.4	182.0	135.6	90.2	–	–	–	–	–
0.6	272.5	193.4	152.5	110.3	71.3	–	–	–	–432.4	–432.4
0.5	249.4	169.9	131.3	93.0	59.0	–	–432.4	–432.4	–382.2	–200.4
0.4	218.8	149.0	115.2	81.6	50.9	–432.4	–374.8	–289.6	–205.1	–125.2
0.3	194.9	132.7	102.5	72.7	44.7	–400.1	–272.5	–210.5	–149.2	– 91.1
0.2	175.7	119.7	92.5	65.5	40.0	–314.4	–214.2	–165.5	–117.2	– 71.6
0.1	159.9	108.9	84.2	59.6	36.4	–258.9	–176.4	–136.3	– 96.5	– 58.9
0.0	146.2	99.9	77.2	54.7	33.4	–220.1	–149.9	–115.8	– 82.1	– 50.1
–0.1	137.5	93.7	72.4	51.3	31.3	–191.4	–130.4	–100.7	– 71.4	– 43.6
–0.2	129.5	88.2	68.1	48.3	29.5	–169.3	–115.3	– 89.1	– 63.1	– 38.5
–0.3	122.5	83.3	64.4	45.6	27.8	–151.8	–103.4	– 80.0	– 56.6	– 34.6
–0.4	115.8	78.9	61.0	43.2	26.4	–137.6	– 93.7	– 72.4	– 51.3	– 31.3
–0.5	110.0	75.0	57.9	41.0	25.1	–125.8	– 85.7	– 66.2	– 46.9	– 28.6
–0.6	104.8	71.4	55.2	39.1	23.9	–115.8	– 78.9	– 61.0	– 43.2	– 26.4
–0.7	100.0	68.1	52.7	37.3	22.8	–107.4	– 73.1	– 56.5	– 40.0	– 24.4
–0.8	95.7	65.2	50.4	35.7	21.8	–100.0	– 68.1	– 52.7	– 37.3	– 22.8
–0.9	91.7	62.5	48.3	34.2	20.9	– 93.7	– 63.8	– 49.3	– 34.9	– 21.3
–1.0	88.0	60.0	46.3	32.8	20.0	– 88.0	– 60.0	– 46.3	– 32.8	– 20.0

NOTES

1 The ratio of f_{Min}/f_{Max} is positive or negative respectively if the maximum and minimum stresses are of like or unlike sign.

2 The value given above include the maximum working stresses for all steels including those of strength higher than that conforming to IS 8500.